THE EFFECT OF INSULIN SENSITIVITY ON CORTICOLIMBIC RESPONSES TO METABOLIC AND VISUAL FOOD CUES

by

Hanin Mohammed Alsaadi

A thesis submitted to the Department of Biomedical and Molecular Sciences (Physiology Graduate Program)

In conformity with the requirements for

the degree of Master of Science

Queen's University

Kingston, Ontario, Canada

(May, 2015)

Abstract

Insulin is one of several molecules that signals the energy balance state to the brain. This study examined the effect of insulin sensitivity on the responsiveness of appetite regulatory brain regions to visual food cues. Nineteen participants diagnosed with polycystic ovary syndrome (PCOS) were studied. Subjects were divided into insulin-sensitive (n=8) and insulin-resistant (n=11) groups based on the homeostatic model assessment of insulin resistance (HOMA2-IR). Subjects underwent functional magnetic resonance imaging (fMRI) while viewing food pictures following water or dextrose consumption. The corticolimbic **B**lood **O**xygen **L**evel **D**ependent (BOLD) responses to high-calorie (HC) or low-calorie (LC) food pictures were compared within and between groups. BOLD responses to food pictures were reduced during a glucose challenge in numerous corticolimbic brain regions of insulin-sensitive subjects, but not in insulin-resistant subjects. In addition, a positive interaction was detected between insulin sensitivity and condition. Furthermore, the degree of insulin resistance positively correlated with the corticolimbic BOLD response in the medial prefrontal cortex (mPFC), orbitofrontal cortex (OFC), anterior cingulate and ventral tegmental area (VTA) in response to HC pictures and in the dorsolateral prefrontal cortex (DLPFC), mPFC, anterior cingulate, and insula in response to LC pictures following a glucose challenge. The activity in the OFC, midbrain, hippocampus, and amygdala was positively correlated with HOMA2-IR in response to HC>LC pictures following a glucose challenge. We conclude that the normal inhibition of corticolimbic brain responses to food pictures during a glucose challenge is compromised in insulin-resistant subjects. The increase in brain responsiveness to food pictures during postprandial hyperinsulinemia may lead to greater non-homeostatic eating and perpetuate obesity in insulin-resistant subjects. Understanding how insulin sensitivity affects appetite-regulating brain regions responses to food pictures is necessary for the

development of prevention strategies and effective therapeutic targets for the treatment of obesity, particularly obesity related to insulin resistance in PCOS.

Co-Authorship

Dean A. Van Vugt, Alicja Krzemien, Hanin Alsaadi, Stephanie Palerme and Robert L. Reid "Effect of insulin sensitivity on corticolimbic responses to food picture in women with polycystic ovary syndrome." *Obesity* (2012). (Van Vugt *et al.*, 2012).

Dean A. Van Vugt, Alicja Krzemien, Hanin Alsaadi, Tamar C. Frank, Robert L. Reid "Glucose-induced inhibition of the appetitive brain response to visual food cues in polycystic ovary syndrome patients." *Brain Research* (2014). (Van Vugt *et al.*, 2014).

Acknowledgements

I would like to express my sincere gratitude to my supervisor, Dr. Dean Van Vugt, for his patience, knowledge, guidance, and support. His guidance and constructive feedback helped me develop a deeper understanding of the field and improved my independent research skills. He was always approachable and willing to help me through all stages of my research. His unique manner of combining discipline with friendliness allowed me to be more productive in a comfortable and collaborative environment. I would also like to express my heartfelt thanks the lab's research assistant, Dr. Alicja Krzemien, for providing me with resources and insightful suggestions along the way and for being a great friend. I have been blessed with Dr. Krzemien's continuous support and help during stressful times. I would also like to thank Dr. Robert Reid for successfully assessing and recruiting study participants to carry out this exciting and important project. I would like to further extend my appreciation to our study participants for their cooperation and punctuality and to the MRI facility at Queen's University for assuring the quality of the data collected.

I would also like to acknowledge the financial support from the Physicians Services Incorporated, the Botterell Foundation, and the Canadian Foundation for Women's Health. The generous financial support from the King Saud Bin Abdulaziz University for Health Sciences that has made it possible for me to have this wonderfully rich academic experience is also greatly appreciated. Outside of university, I have been fortunate to have a number of great friends who created a family-like environment for me. I would like to thank all of them for the encouragement they have provided me throughout this process. Most of all, I am deeply grateful to have a wonderful, supportive and caring family who inspire me to succeed. I am especially indebted to my parents, Mohammed and Horyah, and to my sisters for their unconditional support and love

throughout my studies. To them, I dedicate this thesis. Finally, my humble gratitude goes to God for giving me the strength to complete this project.

Table of Contents

Abstract ii
Co-Authorship iv
Acknowledgements v
List of Figures x
List of Tables xi
List of Abbreviations xii
Chapter 1 Introduction 1
1.1 Obesity 1
1.2 Neural control of ingestive behavior 2
1.2.1 Homeostatic control of food intake 2
1.2.2 Non-Homeostatic food intake 5
1.2.3 Corticolimbic brain circuitry 6
1.3 Functional magnetic resonance imaging (fMRI) of networks affecting appetite 9
1.3.1 fMRI technique 9
1.3.2 Neuronal response to food cues 10
1.3.3 The impact of metabolic state on neuronal response to food cues 12
1.3.4 The impact of adiposity on neuronal response to food cues 13
1.3.5 The impact of metabolic cues on neuronal response 15
1.4 The role of insulin in regulating appetite 16
1.4.1 fMRI studies on insulin effects 17
1.5 Thesis Objectives and Hypothesis 18
Chapter 2 Methods 21
2.1 Subject Recruitment 21
2.2 Experimental protocol 22
2.2.1 Pre-scan instructions 22
2.2.2 fMRI procedure 23
2.2.3 Post-scan instructions 24
2.2.4 Calculating insulin sensitivity 25
2.2.5 fMRI data pre-processing 27
2.2.6 fMRI data analysis 28

2.3 Demographic and behavioral data analysis 30
2.3.1 Demographic data 30
2.3.2 Hunger scores 30
2.3.3 Recall test 31
2.3.4 PANAS 31
Chapter 3 Results 32
3.1 Demographics 32
3.2 Behavioral results 32
3.3 BOLD responses to food pictures in insulin-sensitive and insulin-resistant groups 35
3.3.1 Regional activation by food pictures during water condition 35
3.3.2 Regional activation by food pictures during a glucose challenge 35
3.3.3 Effects of water vs. glucose condition on brain activation by food pictures 41
3.4 Group differences in BOLD responses to food pictures 41
3.4.1 Insulin-sensitive vs. insulin-resistant subjects during water condition 41
3.4.2 Insulin-sensitive vs. insulin-resistant subjects during a glucose challenge 48
3.5 Interaction between insulin sensitivity and study condition 52
3.6 Correlation between insulin resistance and corticolimbic BOLD response to food pictures 55
3.6.1 Correlation between insulin resistance and BOLD response to food pictures during water condition 55
3.6.2 Correlation between insulin resistance and BOLD response to food pictures during a glucose challenge 55
3.6.3 Correlation between insulin resistance and BOLD response to food pictures during glucose vs. water condition 60
Chapter 4 Discussion 64
4.1 Key findings in the current study 64
4.1.1 fMRI results 64
4.2 Contrasting the current study with previous neuroimaging studies 64
4.2.1 Brain reactivity to food cues following a glucose challenge 64
4.2.2 Neuroimaging studies of insulin resistance 66
4.2.3 Is it glucose or insulin that affects brain activity? 67

4.3 The effect of metabolic condition and adiposity 71
4.3.1 Neuroimaging studies in fasted vs. fed in normal weight subjects 71
4.3.2 Neuroimaging studies in fasted vs. fed in normal weight vs. obese 71
4.3.3 Is the brain response due to adiposity or insulin sensitivity? 73
4.4 Study strengths, limitations and future directions 74
4.4.1 Study strengths 74
4.4.2 Limitations 74
4.4.3 Future directions 75
4.4.4 Final remarks 76
References 77
Appendix A 92
Appendix B 94
Appendix C 96
Appendix D 98

List of Figures

Figure 1: Schematic representation depicting the interaction between homeostatic and non-homeostatic appetite regulating centers to influence food intake 4
Figure 2: BOLD signal change over time and the hemodynamic response function 11
Figure 3: Schematic representation of the study hypothesis 20
Figure 4: Experimental paradigm 26
Figure 5: BOLD response in the amygdala, fusiform, OFC and insula in insulin-sensitive and insulin-resistant subjects during a glucose challenge 45
Figure 6: BOLD response in the caudate, fusiform, mPFC, AC, and DLPFC in insulin-sensitive and insulin-resistant subjects during a glucose challenge 46
Figure 7: Interaction between insulin sensitivity and condition 54
Figure 8: Correlation between insulin resistance and BOLD response in the mPFC, OFC, AC and VTA during a glucose challenge 61

List of Tables

Table 1 Clinical and biochemical features of study subjects 33
Table 2 Effect of condition, food picture exposure and insulin sensitivity on hunger 34
Table 3 Effect of type of food pictures and condition on recall test 36
Table 4 Effect of insulin sensitivity and condition on PANAS 37
Table 5 Differential BOLD response to food pictures during water condition in insulin-sensitive and insulin-resistant groups 38
Table 6 Differential BOLD response to food pictures during a glucose challenge in insulin-sensitive and insulin-resistant groups 42
Table 7 Differential BOLD response to food pictures after water vs. glucose condition in insulin-sensitive and insulin-resistant groups 47
Table 8 Group differences in the BOLD response to food pictures during water condition 49
Table 9 Group differences in the BOLD response to food pictures during a glucose challenge .. 50
Table 10 Interaction between insulin sensitivity and condition 53
Table 11 Correlation between insulin resistance and BOLD response to food pictures during water condition 56
Table 12 Correlation between insulin resistance and BOLD response to food pictures during a glucose challenge 57
Table 13 Correlation between insulin resistance and BOLD response to food pictures during glucose vs. water condition 62

List of Abbreviations

AgRP – agouti-related peptide

ARC – arcuate nucleus

BBB – blood-brain barrier

BMI – body mass index

BOLD – blood oxygen level dependent

C – control

CART – cocaine-amphetamine regulated transcript

CNS – central nervous system

CSF – cerebrospinal fluid

DeoxyHb – deoxyhemoglobin

DLPFC – dorsolateral prefrontal cortex

EAT-26 – Eating Attitudes Test-26

fMRI – functional magnetic resonance imaging

FWE – family-wise error

GLP-1 – glucagon-like peptide-1

HC – high-calorie

HOMA2-IR – Homeostatic Model of Assessment of Insulin Resistance 2

ICV – intracerebroventricular injection

ID – Insulin Detemir

LC – low-calorie

MCLD – mesocorticolimbic dopamine pathway

MEG – magnetoencephalography

MNI – Montreal Neurological Institute

mPFC – medial prefrontal cortex

NAc – nucleus accumbens

NPH – Neutral Protamine Hagedorn

NPY – neuropeptide Y

OFC – orbitofrontal cortex

OGTT – oral glucose tolerance test

OxyHb – oxyhemoglobin

PANAS – positive and negative affect schedule

PCOS – polycystic ovary syndrome

PET – positron emission tomography

PFC – prefrontal cortex

POMC – pro-opiomelancortin

PWS – Prader-Willi Syndrome

PYY – peptide YY

PYY3-36 – Peptide YY 3-36

ROI – region of interest

SD – standard deviation

SPM – statistical parametric mapping

SVC – small volume correction

VMPFC – ventromedial prefrontal cortex

VTA – ventral tegmental area

WC – waist circumference

WHO – World Health Organization

Chapter 1

Introduction

1.1 Obesity

Obesity is a multifactorial disease involving an imbalance of energy intake and expenditure (Spiegelman & Flier, 2001). Body mass index (BMI) and waist circumference (WC) are international standards for classifying the health risk associated with increased body weight (WHO). BMI of ≥30 and ≥40 indicate obesity and morbid obesity, respectively. Central obesity is reflected by a WC >102 cm and >88 cm in men and women, respectively (Douketis *et al.*, 2005).

The World Health Organization (WHO) has declared that obesity is an epidemic, estimating that at least 600 million are clinically obese worldwide (World Health Organization, 2015). In Canada, approximately 11.7% of children between the ages of 5 to 17 are obese (Statistics Canada, 2012). This is concerning as childhood obesity is a significant predictor of adult obesity (Whitaker *et al.*, 1997). In the past 25 years, the percentage of individuals considered at high risk of obesity-related health problems has more than doubled among adults aged 40 to 69, and more than quadrupled among adults aged 20 to 39 (Statistics Canada, 2010). Obesity increases the risk of chronic diseases such as diabetes, hypertension, atherosclerosis, osteoarthritis, infertility, and some cancers (Mokdad *et al.*, 2003). In 2014, more than 1.9 billion adults are estimated to be overweight or obese, and most individuals live in countries where overweight and obesity contributes to more deaths than underweight (World Health Organization, 2015). In the US, the costs

associated with obesity are estimated to be $147 billion per year (Finkelstein *et al.*, 2009) and are expected to exceed $500 billion per year by 2030 (Finkelstein *et al.*, 2012).

An obesogenic environment, where there is frequent exposure to highly palatable, low-priced foods, coupled with a sedentary environment, is thought to contribute to obesity (Berthoud *et al.*, 2011). Given the high morbidity, mortality, and cost associated with obesity, much research has focused on developing effective preventative health strategies. A comprehensive understanding of ingestive behavior and appetite regulation will be crucial to developing strategies for preventing, reversing and managing obesity.

1.2 Neural control of ingestive behavior

Human ingestive behavior is regulated by a complex integration of neural and hormonal mechanisms. It is important to consider both homeostatic ingestive behavior, primarily controlled by the hypothalamus and brainstem, and non-homeostatic (hedonic) ingestive behavior, which is thought to be influenced by corticolimbic regions involved in processing pleasure, emotion and reward (Berthoud *et al.*, 2011).

1.2.1 Homeostatic control of food intake

The discovery of leptin, an adipose-derived hormone involved in appetite control and metabolism, was a major breakthrough in obesity research (Zhang *et al.*, 1994). Its discovery prompted investigations into hormones and neuropeptides that affect energy balance (Chicurel, 2000), leading to the identification of many other hormones and neuropeptides that regulate appetite and ingestive behavior. The stimulating factors (orexigens) include hypothalamic neuropeptides such as agouti-related protein (AgRP), neuropeptide-y (NPY), endocannabinoids, melanin concentrating hormone, orexin, and endogenous opioids. Endogenous opioids are also found in the brainstem and pituitary.

Peripheral orexigenic peptides include ghrelin, which is found in the stomach, and adiponectin, which is found in the adipose tissue. In contrast, inhibiting factors (anorexigens) include several gut-derived hormones such as cholecystokinin, which is mostly found in the small intestines, peptide YY 3-36 (PYY3-36), which is found in the L cells of the lower gastrointestinal tract, glucagon-like peptide-1 (GLP-1), which is found in the pancreas and large intestines, leptin, which is released by the adipose tissue, and insulin and amylin, which are found in the pancreas. These peripheral peptides exert their effects on the hypothalamic arcuate nucleus (ARC) directly or indirectly via the circumventricular organs (Fry *et al.*, 2007; Wren & Bloom, 2007). Hypothalamic anorexigenic neuropeptides include cocaine-amphetamine regulated transcript (CART), corticotropin-releasing hormone, and α-melanocyte stimulating hormone (α-MSH), a product of pro-opiomelanocortin (POMC), and nesfatin (Havel, 2001; Suzuki *et al.*, 2011; Sam *et al.*, 2012).

The hypothalamus plays a key role in maintaining energy homeostasis (Figure 1). Within the hypothalamus, the ARC is situated in close proximity to the median eminence, a region lacking the ααblood-brain barrier, facilitating response to appetite regulating hormones (Broadwell & Brightman, 1976). The ARC contains peptidergic neurons that co-express anorexigenic peptides α-MSH and CART and a second population of neurons that co-express orexigenic peptides NPY and AgRP (Cone *et al.*, 2001).

Inhibitory synaptic communication between these neuronal populations ensures a coordinated response (Broberger *et al.*, 1997; Elmquist *et al.*, 1998; Elias *et al.*, 1999; Schulingkamp *et al.*, 2000). Neurons in the ARC mediate peripheral signals related to appetite and satiety, possessing receptors that respond to and integrate various acute and

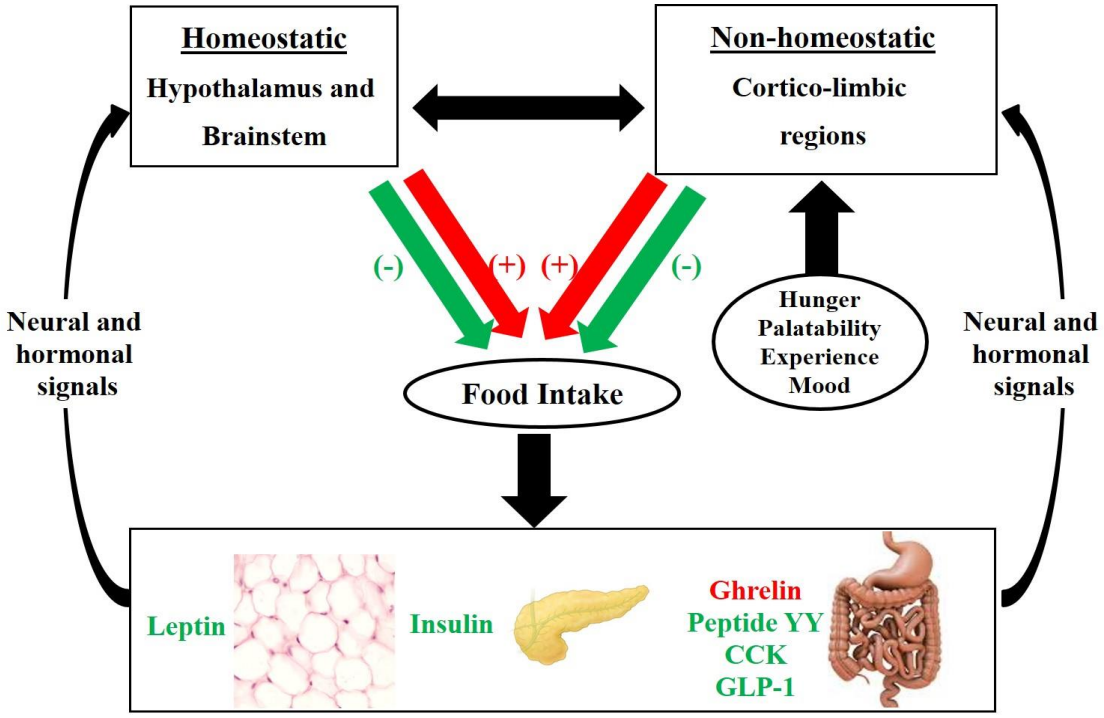

Figure 1: Schematic representation depicting the interaction between homeostatic and non-homeostatic appetite regulating centers to influence food intake

Hormones from adipose tissue and the gastrointestinal tract affect food intake through homeostatic (hypothalamus and brainstem) and non-homeostatic (corticolimbic) brain regions. Significant influences on the corticolimbic pathway include hunger level, food palatability, experience, and mood. Red font indicates appetite stimulator; green font indicates appetite inhibitor. Red arrow indicates stimulation/increase; green arrow indicates inhibition/decrease. Modified from (Van Vugt, 2010).

chronic metabolic signals such as leptin (Mercer *et al.*, 1996), insulin (Schulingkamp *et al.*, 2000), PYY and GLP-1 (Christophe, 1998), and ghrelin (Zigman *et al.*, 2006). During a fed (positive energy) state, the release of appetite inhibitors such as leptin, insulin, PYY3-36, and GLP-1 is increased, while the release of appetite stimulators is decreased. Consequently, appetite inhibitors stimulate anorexigenic neurons that co-express α-MSH and CART and inhibit orexigenic neurons that co-express NPY and AgRP. During a fasted (negative energy) state, ghrelin levels increase and appetite inhibitors decrease, thereby stimulating NPY- and AgRP-expressing neurons while inhibiting neurons that co-express POMC and CART (Schwartz *et al.*, 1996; Schwartz *et al.*, 1997; Elias *et al.*, 1998; Baskin *et al.*, 1999; Elias *et al.*, 1999; Cowley *et al.*, 2001; Halatchev *et al.*, 2004).

Feeding behavior is also regulated by peripheral neural signals. Gastrointestinal vagal and spinal afferents relay mechano-chemical information about nutrient availability in the gut to influence central nervous system (CNS) control of feeding and terminate food consumption (Havel, 2001; Powley & Phillips, 2004; Cummings & Overduin, 2007). Gut peptides convey hunger and satiety signals to the CNS via receptors expressed on visceral vagal afferents (for review see Havel, 2001; Sam *et al.*, 2012).

1.2.2 Non-Homeostatic food intake

There is increasing evidence that brain regions implicated in reward and cognition affect ingestive behavior (Figure 1). The pleasure and reward associated with taste, smell, sight, and texture of food drives eating even in positive energy states, despite the presence of anorexigenic signals or the absence of orexigenic signals. This reaction may delay meal termination or lead to overconsumption of palatable food, resulting in weight gain. This type of ingestive behavior is referred to as non-homeostatic or hedonic eating. Previous

studies have shown that non-homeostatic eating can override homeostatic regulation mechanisms that normally respond to internal metabolic signals of energy excess (Berthoud *et al.*, 2011).

Animal and human research suggest parallels between eating and several addictive behaviors such as smoking, alcohol consumption, and drug abuse (Del Parigi *et al.*, 2003; Pelchat *et al.*, 2004; Simansky, 2005; Volkow & Wise, 2005; Tang *et al.*, 2012). Research utilizing neurophysiological recording, brain stimulation, and brain imaging has suggested that food, nicotine, alcohol, cocaine and amphetamine cues may trigger common neural reward circuits (Wang *et al.*, 2001; Risinger *et al.*, 2005; Stoeckel *et al.*, 2008; Tang *et al.*, 2012). Research evidence and clinical evidence supports the idea that a considerable percentage of the population is unable to improve their eating habits despite being informed about the negative consequences of obesity. Notwithstanding the impressive list of energy balance signals and their contribution to homeostatic regulatory mechanisms, achieving or maintaining energy homeostasis and restricting appetite is difficult for a large segment of society. The ability of environmental and behavioral influences to so profoundly affect the human metabolic state suggests that this exquisite homeostatic control system is being over-ridden by brain regions that respond to cognitive, emotional, and reward-based processing of food cues (corticolimbic brain regions) (Carnell *et al.*, 2012). The interaction between homeostatic and non-homeostatic brain regions and the location of hormones involved in the regulation of food intake is summarized in (Figure 1).

1.2.3 Corticolimbic brain circuitry

Corticolimbic regions constitute a neural network involved in learning, memory, taste, emotion, motivation and goal-directed behavior (Berthoud *et al.*, 2011). These regions

appear to be responsive to appetitive stimuli, assigning reward values and converting these to initiate actions (Berthoud *et al.*, 2011). The corticolimbic pathway is comprised of limbic, cortical and subcortical structures. These regions include the prefrontal cortex (PFC), lateral and medial orbitofrontal cortex (OFC), anterior cingulate, insula, hippocampus, amygdala, ventral striatum/nucleus accumbens (NAc), dorsal striatum (caudate and putamen), pallidum, ventral tegmental area (VTA) and fusiform gyrus (Fulton, 2010). The limbic structures include the amygdala, cingulate gyrus, thalamus, hypothalamus, parahippocampal gyrus and hippocampus (Haber & Knutson, 2010). Of these, the amygdala, cingulate, thalamus and hypothalamus have been implicated in processing appetitive and aversive motivation and memory (Fulton, 2010). The amygdala is involved in emotion and fear processing, and emotional aspects of sensory information (Schoenbaum *et al.*, 1998; Baxter & Murray, 2002). Projections from cortical, subcortical and limbic regions intersect in the amygdala, which receives somatosensory, olfactory, visual, auditory, gustatory and visceral efferents directly and indirectly from cortical and subcortical regions (Sah *et al.*, 2003). The amygdala also receives direct inputs from the hippocampus and sends outputs through the entorhinal cortex to the hippocampus. The hippocampus plays a critical role in learning and memory formation, as well as sensorimotor and motivational processing (Bast & Feldon, 2003; Wittmann *et al.*, 2005; Wallner-Liebmann *et al.*, 2010).

The PFC integrates cognitive and emotional information, and is involved in reward evaluation, inhibitory control, executive decision making and suppression of inappropriate responses (Watanabe, 1996; Cardinal *et al.*, 2002; Hare *et al.*, 2009). The dorsolateral PFC (DLPFC) plays a major role in reward anticipation, behavioral outcome prediction, and

executive self-control (Miller, 1999; Hare *et al.*, 2009). The medial PFC (mPFC) helps facilitate emotional, memory and higher-order sensory processing, and signals a stimuli's emotional value (Cardinal *et al.*, 2002; Hare *et al.*, 2009). The ventromedial PFC (VMPFC) is implicated in reward evaluation (including pleasantness of food) and cognitive processing, such as emotion-related learning and behavior, and decision making (Watanabe, 1996; Hare *et al.*, 2009). The VMPFC includes the OFC and the secondary gustatory cortex, which receives afferents from all sensory modalities via the thalamus and somatosensory cortex, and sends efferents to cortical, subcortical and limbic structures to assign reward values to stimuli (Rolls *et al.*, 1980; Schoenbaum *et al.*, 1998; Rolls & McCabe, 2007; Sescousse *et al.*, 2010; Barbas *et al.*, 2011; Rolls, 2011).

Another critical pathway implicated in the processing of reward and pleasure is the mesocorticolimbic dopamine (MCLD) pathway. The MCLD pathway influences eating behavior by regulating mood, pleasure and desire. The MCLD pathway originates in the midbrain VTA and the zona compacta of the substantia nigra and sends dopaminergic projections to cortical and subcortical structures (Fulton, 2010; Stice *et al.*, 2011; Baik, 2013).

The dorsal striatum plays a role in association learning involving sensory stimuli, and in deciding on appropriate actions or reactions to those stimuli based on subsequent rewards (Koob & Volkow, 2009). The ventral striatum/NAc is part of the basal ganglia and is involved in mesolimbic dopamine circuitry. It receives dopaminergic inputs that relay reward and pleasure-related information from the VTA (Esch & Stefano, 2004; Fulton, 2010; Stice *et al.*, 2011). It is hypothesized that the NAc has a function in mediating food reward and pleasure, as well as goal-directed behavior (Tang *et al.*, 2012). The NAc is

thought to integrate homeostatic and non-homeostatic regulatory signals by receiving inputs from the hypothalamus and sending projections to higher corticolimbic regions such as the PFC and the insular cortex (Kelley, 2004). Furthermore, the anatomical organization of the NAc suggests that it serves as a neural bridge between the corticolimbic and motor systems, thus allowing the convergence of affective and motivational inputs into motor actions (Mogenson *et al.*, 1980; Kelley, 2004; Hare *et al.*, 2009). It has been suggested that the interaction between homeostatic and non-homeostatic processes that regulate appetite and ingestive behavior is partly mediated by the NAc (Zahm, 2000).

The insula (primary gustatory cortex), located within the brain's lateral sulcus, is divided into two functionally distinct areas. The anterior insula receives and integrates information from the VTA, NAc, amygdala, striatum, and OFC for taste and texture discrimination and assigns hedonic value to food. The posterior insula conveys visceral and gustatory signals related to gastric distension, pain, and temperature from the NTS and the parabrachial nucleus to sensory areas (Small, 2006; Tomasi *et al.*, 2009; Cauda *et al.*, 2011; Frank *et al.*, 2013). Lastly, the fusiform gyrus is a key area involved in visual processing and object recognition (Fulton, 2010). For a comprehensive review of the functional neuroanatomy of corticolimbic regions see (Morgane *et al.*, 2005; Haber & Knutson, 2010).

1.3 Functional magnetic resonance imaging (fMRI) of networks affecting appetite

1.3.1 fMRI technique

Functional magnetic resonance imaging (fMRI) is a noninvasive and indirect method for quantifying brain activity by measuring the blood oxygen level dependent (BOLD) signal. The BOLD signal results from the changes in the ratio of oxyhemoglobin (oxyHb)

to deoxyhemoglobin (deoxyHb) over time. The hemodynamic response increases to meet the increased metabolic demand of active cells, which increases the oxyHb to deoxyHb ratio (Aguirre *et al.*, 1998). These changes are detected by the MRI scanner (Ogawa *et al.*, 1990; Arthurs & Boniface, 2002; Logothetis & Wandell, 2004; Nair, 2005). MRI scanners produce brain images (maps) with high spatial (1 mm) and temporal (1 second) resolution, allowing researchers to study the rapid and dynamic changes in metabolic demand of active regions in response to experimental stimuli (Huettel *et al.*, 2004; Lindquist, 2008).

The BOLD response consists of three phases (Figure 2). The first phase, marked by the initial dip, results from an increase in neuronal activity due to the experimental task, causing an increase in oxygen metabolism. This decreases local oxyHb levels and increases local deoxyHb levels (Malonek & Grinvald, 1996). To provide the active region with oxygen and nutrients, cerebral blood flow increases approximately 2 seconds following the stimulus, peaks between 4 and 6 seconds, and results in the increase of the oxyHb to deoxyHb ratio (second phase). Subsequently, there is a prolonged dip, which results from a decrease of the oxyHb to deoxyHb ratio (third phase). In the absence of a stimulus, oxyHb and deoxyHb levels return to normal (Huettel *et al.*, 2004; Lindquist, 2008).

1.3.2 Neuronal response to food cues

fMRI technology has been used to study appetite regulation in humans. Brain responses to metabolic signals and visual food cues are providing new information about homeostatic and hedonic regulation of ingestive behavior. Various food-related cues, such as images of food, have been used to elicit neural responses because of ease of delivery and ability to signal the potential availability of food, which stimulates reward circuits and may affect motivation/desire to eat (St-Onge *et al.*, 2005). fMRI studies have consistently shown that

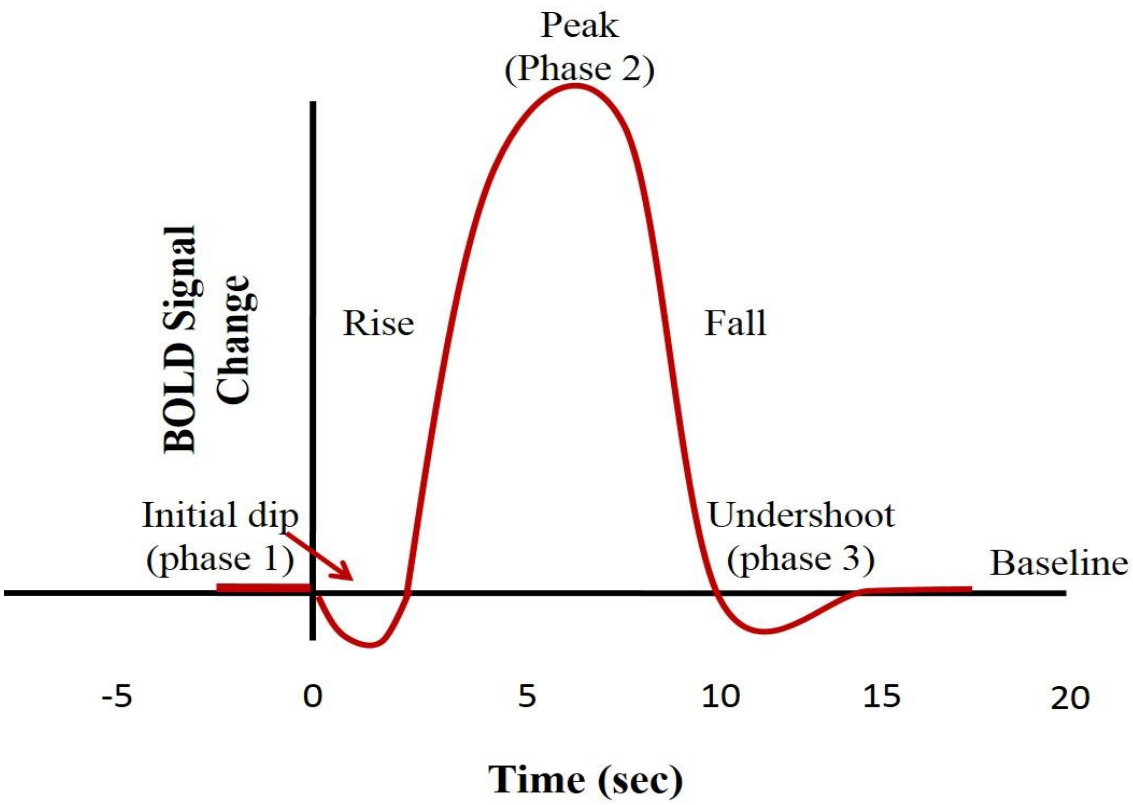

Figure 2: BOLD signal change over time and the hemodynamic response function

Phase 1 represents an increase in neuronal activity, leading to an increase in normal oxygen metabolism and deoxygenated hemoglobin (deoxyHb). Phase 2 reflects an increase in cerebral blood flow, leading to an increase in oxygenated hemoglobin (oxyHb) and a decrease in deoxyHb. In phase 3, there is a reduction in cerebral blood flow, leading to increase in deoxyHb and a decrease in oxyHb. In the absence of a stimulus, oxyHb and deoxyHb levels return to baseline. Modified from (Lindquist, 2008).

the BOLD response to visual food cues is most pronounced in corticolimbic brain regions such as PFC, lateral and medial OFC, amygdala, hippocampus, parahippocampus, anterior cingulate, insula, hypothalamus, striatum, pallidum, VTA, and fusiform (Van der Laan *et al.*, 2011; Huerta *et al.*, 2013).

Many variables have been shown to significantly influence the BOLD response to food stimuli, including hunger, adiposity, mood, stimulus salience, gender, and personality. Salience of the stimulus is a particularly important variable influencing the BOLD response. For instance, fMRI studies examining responses to food pictures of different motivational salience found differential responses to high-calorie (HC), low-calorie (LC), and control (C) pictures in healthy, normal weight individuals. HC food pictures increased the BOLD signal in the lateral OFC, hypothalamus, inferior temporal visual cortex, posterior parietal cortex, premotor cortex and hippocampus (Killgore *et al.*, 2003; Cornier *et al.*, 2007), whereas LC food pictures produced less activation in the medial OFC and insular cortex. These studies suggest that, compared to food with lower hedonic value, attention and motivation to eat food of high hedonic value may be increased in normal weight individuals.

1.3.3 The impact of metabolic state on neuronal response to food cues

Functional imaging studies have investigated the differences in brain responses to food cues under fasted and fed conditions in normal weight and obese individuals. An fMRI study found that healthy women who fasted for 18 hours showed a greater BOLD response to HC than LC food pictures in the posterior cingulate cortex, medial OFC, insula, caudate, putamen and fusiform gyrus. Conversely, when these women were fed a 500 kcal lunch, they showed a greater BOLD response to LC than HC food pictures in the same regions

(Siep *et al.*, 2009). A study using fMRI to examine the corticolimbic regions involved in hunger (after a 14-hour fast) and satiation (after ad libitum ingestion of a mixed meal) found that fasted subjects had increased activity in the insula, striate and extrastriate cortex, anterior midprefrontal cortex, thalamus, cerebellum, inferior parietal lobes and cingulate cortex in response to food pictures (Fuhrer *et al.*, 2008).

An fMRI study in normal weight individuals found that food pictures elicited a greater BOLD response in the posterior parietal cortex, inferior temporal visual cortex, premotor cortex, hippocampus and hypothalamus after two days of a eucaloric diet as compared to after two days of overeating (Cornier *et al.*, 2007). This attenuation of BOLD responses to food pictures in regions that are related to visual processing of, and attention to, food pictures, reward evaluation and regulation of energy intake after two days of overeating suggests that normal weight individuals are sensitive to satiety signals associated with feeding. Collectively, these neuroimaging studies reveal a decrease in brain responsiveness to food cues in a satiated compared to a fasted state in healthy, normal weight individuals.

1.3.4 The impact of adiposity on neuronal response to food cues

Researchers have also studied the differences in brain responses to food cues in normal weight, overweight, obese and morbidly obese individuals in varying energy states to identify neural substrates that contribute to overeating or are affected by adiposity. Two studies compared BOLD responses to HC, LC and C pictures between normal weight and obese women (Rothemund *et al.*, 2007; Stoeckel *et al.*, 2008). Both studies found that HC pictures led to enhanced activation in the lateral OFC, insula, hippocampus and cingulate compared to LC or C pictures, and that this difference was greater in the obese vs. normal weight group. Stoeckel *et al.* also reported activation in the medial OFC, amygdala,

NAc/ventral striatum, mPFC, ventral pallidum, caudate and putamen. The greater response was attributed to subjects feeling hungry. This conclusion is supported by the finding that food pictures have greater salience in a fasted vs. fed state and suggests that highly palatable, HC food may increase obese peoples' attentiveness and motivation to ingest food (Rothemund *et al.*, 2007; Stoeckel *et al.*, 2008).

Martin *et al.* compared brain responses to food pictures in obese and normal weight subjects before and after eating. Subjects underwent two scanning sessions: in the pre-meal, unfed condition (after a 4-hour fast) and in the post-meal (fed) condition (after a 500 kcal meal); the order of the sessions was counterbalanced across subjects to minimize the effect of novelty during the first scan. Under the fasted condition, the obese group showed a greater BOLD response to food pictures in the mPFC, anterior cingulate and frontal gyrus compared to the normal weight group. After eating, the obese group also showed a greater increase in the BOLD response to food pictures in the mPFC, caudate, hippocampus and superior frontal gyrus compared to the normal weight group (Martin *et al.*, 2009). Similarly, studies performed in subjects with Prader-Willi Syndrome (PWS), a rare genetic disorder characterized by insatiable appetite and hyperphagia that results in early onset of extreme obesity, also showed a hyperactive corticolimbic response to visual food cues. Patients compared to normal weight subjects, exhibited greater activation of the amygdala, OFC, insula, parahippocampus, and fusiform when scanned immediately after eating a standardized meal (Holsen *et al.*, 2006).

Collectively, these studies show that compared to normal weight individuals, obese individuals show greater activation to food cues in several brain regions, including reward

related regions, under both fasted and fed conditions. This suggests that obese individuals may have altered brain responses to satiety signals.

1.3.5 The impact of metabolic cues on neuronal response

fMRI has also been used to study the effects of nutrients, gut-derived hormones, and adipose tissue-derived hormones on the brain (Gibson *et al.*, 2010). In a study using resting state fMRI with lean and obese individuals, BOLD signal was reduced by 8% in the ventromedial nucleus, an area that promotes eating, in lean subjects 4-10 minutes after ingestion of an oral glucose solution after a 12 hour fast. However, in obese subjects this inhibitory response was smaller and slower, suggesting that obesity is accompanied by a reduction in hypothalamic responsiveness to satiety cues (Matsuda *et al.*, 1999). Similarly, further studies in humans and rats found that a glucose challenge reduced BOLD signal in the hypothalamus in a dose dependent manner (Liu *et al.*, 2000; Mahankali *et al.*, 2000; Smeets *et al.*, 2005). Administering ghrelin to normal weight subjects increased the activity in OFC, PFC, amygdala, insula and striatum in response to food pictures (Malik *et al.*, 2008). The authors suggested that the BOLD signal and behavioral effects of ghrelin were related since the response magnitude in the OFC and amygdala correlated with the increased hunger levels elicited by ghrelin.

fMRI studies have also measured the effect of leptin on BOLD responses to visual food cues in leptin-deficient patients. An fMRI study found that food pictures elicited a greater BOLD response in the insula, parietal lobe, and striatum, as well as increased hunger ratings when patients were not undergoing leptin therapy, as compared to when they were (Farooqi *et al.*, 2007). When patients underwent leptin replacement therapy, PFC activity increased and hunger ratings decreased (Baicy *et al.*, 2007). Another study examined brain

responses to visual food cues before and after obese patients underwent a 10% reduction in body weight (Rosenbaum *et al.*, 2008). The presentation of visual food cues to patients post-weight loss, when leptin levels were lower, caused more activity in the brainstem, culmen, parahippocampal gyrus, inferior and middle frontal gyri, middle temporal gyrus, and lingual gyrus, but decreased activity in the hypothalamus, cingulate gyrus, and middle frontal gyrus, compared to pre-weight loss state, when leptin levels were relatively high. When leptin levels were returned to pre-weight loss levels using exogenous leptin, these responses were reversed, suggesting that these brain areas are highly responsive to altered leptin concentrations (Rosenbaum *et al.*, 2008).

Batterham *et al.* investigated how PYY affects brain activity using resting state fMRI. Subjects were scanned on two occasions (7 days apart) in a counterbalanced order while infused with PYY or saline. Subjects were provided with unrestricted access to a buffet meal 30 minutes after the scan. Fasted subjects infused with PYY3-36 to produce postprandial concentrations of PYY had a strengthened BOLD signal in the caudolateral OFC and a significant reduction in caloric intake post-infusion. The number of calories consumed was inversely proportional to the strength of the BOLD response, suggesting that appetite was inhibited in part by PYY activation of the OFC (Batterham *et al.*, 2007).

1.4 The role of insulin in regulating appetite

The role of insulin in regulating plasma glucose is well documented in the literature. The characteristic postprandial increase in insulin concentration signals an increase in acute energy, while obesity-associated hyperinsulinemia points to a chronic energy state and suggests that surplus energy is being stored (Benoit *et al.*, 2004). Insulin also plays an important role in CNS regulation of appetite (Schulingkamp *et al.*, 2000). Cerebrospinal

fluid (CSF) insulin concentrations parallel post-meal changes in plasma insulin concentrations in rats, revealing the ability of insulin to cross the blood-brain barrier (BBB) (Strubbe *et al.*, 1988). Insulin receptors are widely distributed in brain regions that regulate homeostatic and non-homeostatic food intake. Both insulin receptors and insulin receptor substrate-2 are found in the ARC, and the dorsomedial and ventromedial nuclei, hypothalamic regions well-known to affect food intake (Baskin *et al.*, 1983). Insulin receptors are also present in extra-hypothalamic regions such as the hippocampus, olfactory bulb, cerebral cortex, cerebellum, brainstem, the VTA/SNc, area postrema, medial nucleus of the solitary tract, and in the dorsal motor nucleus of the vagus nerve (Kleinridders *et al.*, 2014). Insulin may act as a physiological inhibitor of food intake via central regulation. This is supported by the fact that intracerebroventricular (ICV) injection of insulin inhibits the hypothalamic expression of NPY in rats (Schwartz *et al.*, 1992). Furthermore, chronic ICV insulin administration inhibited food intake in baboons (Figlewicz *et al.*, 1995) and led to significant weight loss in both baboons and sheep (Woods *et al.*, 1979; Foster *et al.*, 1991). In healthy women, intranasal insulin administration after a meal led to decreased appetite and snack intake (Hallschmid *et al.*, 2012). The most compelling evidence that insulin signaling in the brain inhibits food intake lies in the observation that neuron-specific insulin receptor knockout mice are hyperphagic and develop diet-induced obesity and dyslipidemia (Bruning *et al.*, 2000).

1.4.1 fMRI studies on insulin effects

Recent neuroimaging studies have shown that insulin affects brain response to food cues. An fMRI study investigated the relationship between fasting plasma insulin levels and hippocampal activity in response to HC and LC food pictures in 12 obese and 12

normal weight subjects. They showed that fasting plasma insulin levels, but not BMI, positively correlated with hippocampal activity in response to HC food pictures (Wallner-Liebmann *et al.*, 2010). Another study demonstrated that intranasal insulin administration to healthy participants, which aimed to increase CSF insulin levels while avoiding peripheral effects of insulin, significantly reduced the BOLD signal in the fusiform gyrus, hippocampus, temporal superior cortex, and frontal middle cortex in response to food pictures as compared to placebo (Guthoff *et al.*, 2010). Kroemer *et al*. examined the brain response of normal weight subjects to food pictures following an oral glucose tolerance test (OGTT) and showed that reactivity to food pictures in the fusiform gyrus, superior temporal gyrus, medial frontal gyrus, and limbic system was negatively correlated with insulin but not glucose levels (Kroemer *et al.*, 2012).

Together these studies demonstrate that fMRI is effective in elucidating how appetitive stimuli and energy balance signals influence neural control of appetite and ingestive behavior in humans (Gibson *et al.*, 2010).

1.5 Thesis Objectives and Hypothesis

Polycystic ovary syndrome (PCOS) affects roughly 6.6% reproductive-age women (Lo *et al.*, 2006) and is characterized by oligo-ovulation or anovulation, clinical and/or biochemical evidence of hyperandrogenism, and polycystic ovary morphology (PCOS Consensus Workshop Group, 2004). Women with PCOS often show at least one component of metabolic syndrome (e.g., obesity, dyslipidemia, hypertension or insulin resistance), and the prevalence of obesity (Lo *et al.*, 2006), insulin resistance (Dunaif *et al.*, 1989; Dunaif, 1997; Amanti-Kandarakis & Dunaif, 2012), and type 2 diabetes (Moran *et al.*, 2010) is higher in women with PCOS than in weight-matched women without PCOS.

Since insulin sensitivity in PCOS ranges from normal to resistant, PCOS is an ideal model to address how appetite circuits respond to visual and metabolic cues, and how insulin resistance affects these responses. Thus, the aim of the current study was to determine the effect of insulin sensitivity on the responsiveness of appetite and reward brain regions to food pictures. We used fMRI to compare the corticolimbic BOLD response to HC or LC food pictures in insulin-sensitive and insulin-resistant subjects with PCOS during a glucose challenge or water control. We hypothesized that a glucose challenge would reduce BOLD responses to food pictures in corticolimbic regions normally involved in executive function, reward, emotion and appetite regulation (such as the DLPFC, mPFC, OFC, brainstem (midbrain), caudate, putamen, pallidum, anterior cingulate, insula, hippocampus, amygdala, VTA, NAc, substantia nigra and fusiform) in insulin-sensitive subjects, and that this effect would be compromised in insulin-resistant subjects (Figure 3).

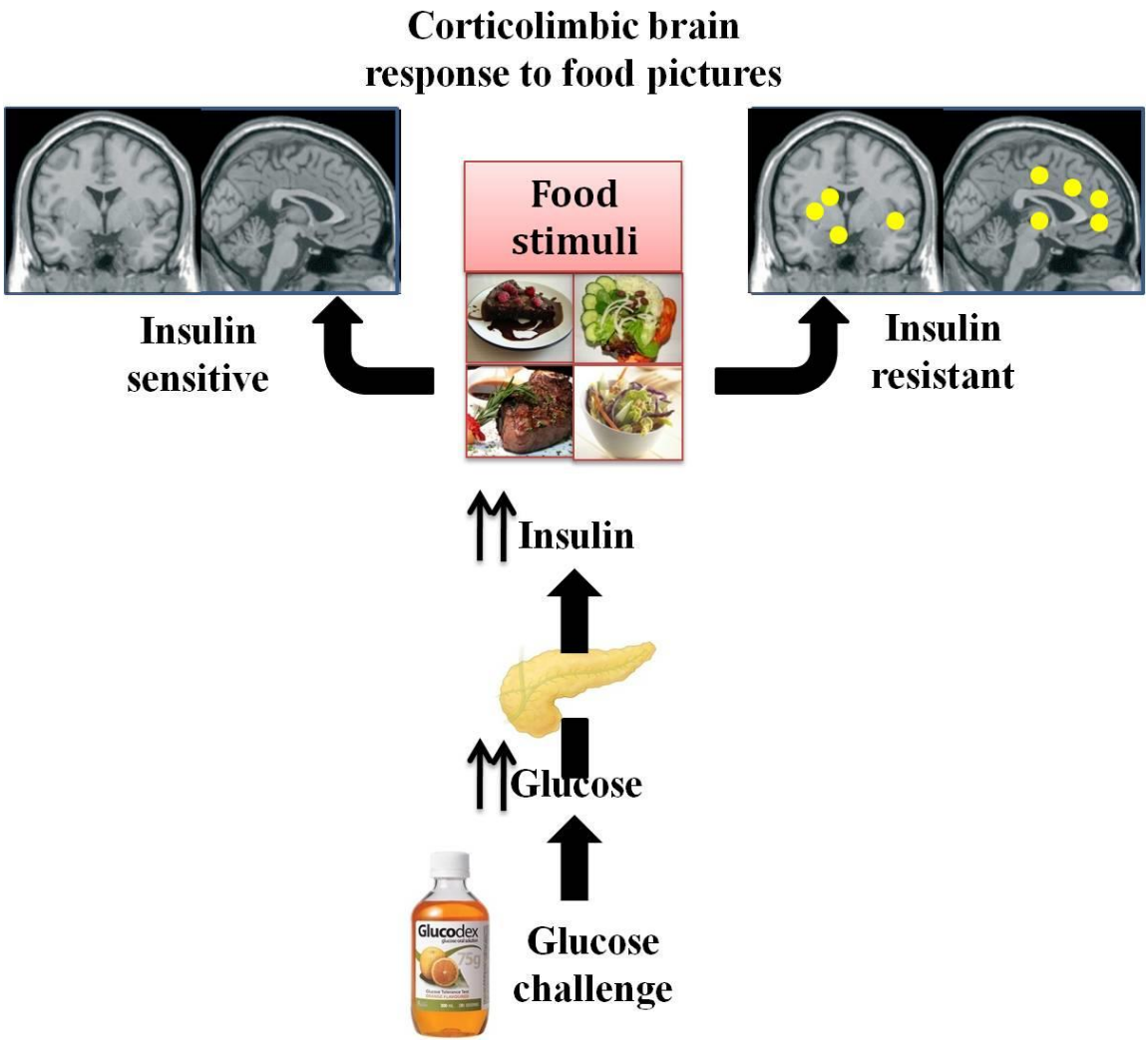

Figure 3: Schematic representation of the study hypothesis

The glucose challenge will lead to increased blood glucose levels and subsequent insulin release. We hypothesized that in insulin-sensitive individuals this would lead to a reduction in the BOLD response to food pictures in corticolimbic regions. We further hypothesized that this effect would be compromised in insulin-resistant subjects who would show an increased BOLD response to food pictures in corticolimbic regions.

Chapter 2

Methods

2.1 Subject Recruitment

Women diagnosed with PCOS between the ages of 18 and 39 years were recruited by local obstetricians and gynecologists and poster advertisements on Queen's University campus and Kingston General Hospital. Both ovulatory dysfunction and hyperandrogenism were required for a diagnosis of PCOS. Ovulatory dysfunction was defined as oligo-ovulation (<8 cycles/year) or secondary amenorrhea. Hyperandrogenism was defined as evidence of hirsutism or acne on clinical exam and/or elevated serum testosterone. The diagnosis of PCOS was made after excluding other etiologies of ovulatory dysfunction or excess androgen. Study exclusion criteria included left-handedness, vegetarianism, claustrophobia, smoking, current or past drug/alcohol abuse, psychoactive medication, history of head injury, or presence of ferromagnetic material in the body. Participants were financially compensated in the amount of $150 upon study completion. All procedures were reviewed and approved by the Queen's University Health Sciences and Affiliated Teaching Hospitals Research Ethics Board.

The subjects completed phone and in-person screening sessions. Subjects were screened for eating disorders with the Eating Attitudes Test (EAT-26) (Garner & Garfinkel, 1979; Garner *et al.*, 1982) (Appendix A). During the orientation, participants were familiarized with the Queen's University imaging center, placed into a sham scanner and given instructions as to what they could expect on scan day to minimize anxiety during the scanning procedure. Written informed consent was obtained from all subjects at this time.

Subjects were given blood work requisitions for fasting insulin, fasting glucose, OGTT, and testosterone measurements. To ensure that subjects were imaged during the follicular phase, scanning sessions were booked one week after a progestin-induced withdrawal bleed (Provera 5 mg for 10 days) for oligo-ovulatory subjects and at earliest convenience for extreme oligo-ovulatory and anovulatory subjects. Twenty PCOS subjects were initially included. One subject was excluded after being diagnosed with type 2 diabetes. As a result, the final analyses were based on 19 subjects.

2.2 Experimental protocol

2.2.1 Pre-scan instructions

Subjects were instructed to eat a normal breakfast before 0900 h on the day of the scan, but to skip lunch and consume only water to ensure a 6-hour fast before the scan. Subjects were scanned between 1400 and 1500 h to minimize potential circadian rhythm effects on appetite. Subjects filled out the Queen's University fMRI facility safety checklist (Appendix B) and a 9-item pre-scanning questionnaire used to assess subjects' mental and physical state (Appendix C). Subjects were told that they would be shown pictures of food while in the scanner and instructed to think about how pleasant it would be to eat the food. In addition, subjects were told of a post-scan picture recall test to motivate them to remain alert while viewing pictures in the scanner. Subjects underwent fMRI scanning sessions on two separate occasions while viewing HC, LC and C pictures: once after drinking water and once after drinking 300 ml water containing 75 g d-dextrose (ratio-GLUCOSE; ratiopharm), in a counterbalanced order. Subjects remained seated for 5 minutes after drinking before being positioned in the scanner. Subjects with extreme oligo-ovulation or amenorrhea (n=12) underwent a second scan session using the same protocol, but after the

alternative treatment (water or glucose) 1-2 weeks later. Seven subjects were scanned 25-72 days after the first due to scheduling conflicts (n=4) or, in subjects with semi-regular periods (n=3), to ensure that both scans were conducted during the mid-follicular phase.

2.2.1.1 Visual stimulation protocol

Subjects were presented with food pictures classified as HC or LC. HC stimuli included pictures of savory, sweet, and high-fat foods such as hamburgers, French fries, pizza, ice cream, and cake (64 pictures in total). LC stimuli included pictures of water and fiber-based foods such as fresh vegetables, fruits, and salads (64 pictures in total). Stimuli of similar colors and complexity consisting of landscapes, buildings, furniture, or household objects not associated with food were included to control for response to visual perception (64 pictures in total). A scanning session consisted of 4 runs each lasting 370 seconds; runs were separated by 30 seconds of rest. The visual stimuli were presented in a block design during the 4 runs. A single run included 12 picture blocks (4 HC, 4 LC and 4 C), each lasting 20 seconds. Four pictures from the same category were presented in each block (4.5 seconds/picture), interspersed with a fixation cross for 0.5 seconds. Blocks were separated by 10 seconds of a blank screen with a central fixation cross (rest). Blocks were presented in pseudo-random order.

2.2.2 fMRI procedure

fMRI experiments were performed in a 3.0 T whole body scanner (Siemens Magnetom Trio Tim syngoMR B15, Erlagen, Germany) equipped with a 12 channel head coil at the Queen University's MRI facility. A three-plane localizer scan, used to ensure proper positioning within the scanner, was followed by acquisition of anatomical scans. The anatomical scan generates high-resolution T1-weighted 3D structural images such that

brain structures can be identified (Magnetization Prepared Rapid Acquisition Gradient Echo, TR (Repetition time) = 1760 ms; TE (echo time) = 2.2 ms; flip angle of 9 degrees; FOV (field-of-view) = 256 mm x 256 mm x 256 mm; voxel size = $1mm^3$).

Functional images were collected as subjects viewed visual stimuli beginning 15 minutes after drinking the solution of glucose or water. Forty-four contiguous slices in the axial plane were acquired by using a T2-weighted echo planar imaging sequence (TR 3000 ms, TE 30 ms, flip angle = 84 degrees; FOV 240 mm x 240 mm, 80 x 80 matrix; voxel size = $3mm^3$, no gap). During the scans, subjects were exposed to the visual stimulus protocol consisting of a set of 192 standardized color pictures previously selected from an Internet search. The image size was adjusted to 1800x1350 pixels and 300dpi using the automatic image adjustment command in Adobe Photoshop (v5.5). The images were presented to subjects using MATLAB v.7.2 2006 software (The Mathworks, Inc., Natick, MA), projected on a screen at the head of the scanner bore and viewed through a mirror mounted on the head coil.

2.2.3 Post-scan instructions

Upon exiting the scanner, subjects completed a 9-item post-scanning questionnaire (Appendix C) identical to the pre-scanning questionnaire. This questionnaire was designed to assess post-scan hunger and well-being, and to determine whether the visual stimuli induced changes in appetite (Appendix C). Since it has been previously shown that mood influences the BOLD response to food pictures (Killgore & Yurgelun-Todd, 2006), mood was assessed by administering the 20-item Positive Affect Negative Affect Survey (PANAS, Appendix D). This survey includes 10 positive emotions (e.g., excited, enthusiastic), and 10 negative emotions (e.g., hostile, guilty). Items were rated on a five-

point scale from 1 (very slightly or not at all) to 5 (extremely). Subjects also completed a recall test administered using the quiz feature in WebCT to ensure that subjects had been attentive to images while in the scanner. The recall test consisted of 4 novel pictures and 4 repeat pictures from each of the 3 categories (24 pictures in total). A correct response was defined as a subject's correct identification that a picture had or had not been viewed during the preceding fMRI scan session. Height, weight, hip and waist circumference (WC) were measured for each subject following the scan.

2.2.4 Calculating insulin sensitivity

To assess insulin sensitivity, a blood sample was collected between 0800 and 0900 after an overnight fast. Plasma insulin concentration was determined using a monoclonal immunoenzymatic assay (Ultrasensitive Insulin Beckman Coulter UniCelDxI 800 Access Immunoassay System). Glucose concentration was measured by the glucose oxidase method using the Beckman Coulter UniCel® DxC 800 SYNCHRON® Clinical System. HOMA2-IR was used as the metric of insulin sensitivity. The HOMA2-IR online calculator v2.2.2 downloaded from http://www.dtu.ox.ac.uk was used to calculate insulin resistance from fasting plasma glucose (mmol/L) and fasting plasma insulin (pmol/L) values. Subjects with a HOMA2-IR score of at least 1.7 were considered to be insulin resistant (Schöfl *et al.*, 2002; Geloneze *et al.*, 2009; Safar *et al.*, 2011; Marsh *et al.*, 2013). Subjects were separated into insulin-sensitive (n=8) and insulin-resistant (n=11) groups (Figure 4). The glucose and insulin measurements were performed between the two fMRI scanning sessions and insulin sensitivity was assessed at the end of the study.

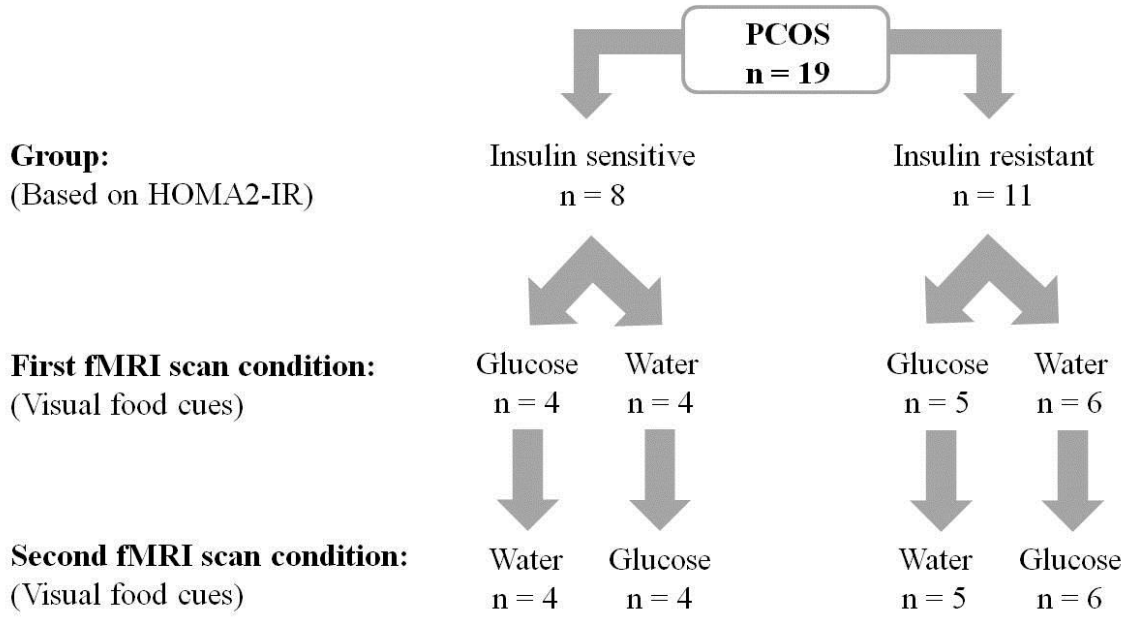

Figure 4: Experimental paradigm

A flow diagram and PCOS patient partitioning of the study. PCOS subjects (n=19) were devided into insulin-sensitive (n=8) and insulin-resistant (n=11) groups according to their insulin sensitivity status. The cutoff levels for insulin resistance was HOMA2-IR≥1.7.

2.2.5 fMRI data pre-processing

Brain scans were preprocessed and analyzed using Statistical Parametric Mapping 8 (SPM8) (Wellcome Dept. Imaging Neuroscience, London, UK) software run in MATLAB v.7.2. (The Mathworks, Inc., Natick, MA). Images acquired by the MRI scanner (DICOM images) were converted into NIFTI format (a format recognized by SPM). To reduce non-steady state effects, the first three functional images from each run were discarded. The remaining functional images underwent a series of pre-processing steps. The functional images were first realigned to correct for movement artifacts during scanning. This was achieved by aligning the functional scans to the first functional image, generating a mean functional image. During coregistration, the mean functional image was overlaid onto the anatomical image. The structural image was then segmented into its different tissue components. Subsequently, the images were normalized by warping the specific tissue components to fit the standard anatomical template. Since subjects in this study were selected from a normal population, scans were normalized to the Montreal Neurological Institute (MNI) standard template brain (ICBM152). The last step entailed smoothing the images, a process that increases the signal-to-noise ratio. A Gaussian kernel of 6 mm full-width-half maximum was used for spatial smoothing. This smoothing parameter was chosen to increase the chance of observing significant activation without sacrificing spatial resolution. To remove low-frequency noise and signal drift, a 128-second high-pass filter was applied. For detailed information on the statistical analyses in statistical parametric mapping in fMRI, readers are referred to the SPM website: http://www.fil.ion.ucl.ac.uk/spm/doc/.

2.2.6 fMRI data analysis

fMRI data sets were analyzed as a block design within the context of the General Linear Model (Monti, 2011). Brain activation was modeled with a boxcar function convolved with the canonical hemodynamic response function, and the goodness of fit of each stimulus-specific regressor was assessed for the BOLD time series in each voxel. First level (fixed-effects) analyses were carried out to yield statistical parametric maps for contrasts of interest by subtracting the response to one picture type (HC, LC or C) from the response to another picture type for each subject. For each subject's control and glucose challenge conditions, the contrasts examined were HC-C, LC-C and HC-LC.

Individual contrast images were incorporated into a second level group-wise (random-effects) analysis using a full factorial design approach in SPM8 to compare the brain responses of insulin-sensitive and insulin-resistant groups. Each group was tested separately using one-sample t-tests to examine the qualitative differences in their responses to pictures of different types of food under water and glucose conditions, as well as to compare their responses to food pictures across conditions. In the latter case, the BOLD response in the glucose challenge condition was subtracted from the BOLD response in the water condition and vice versa (water vs. glucose).

Two-sample t-tests were used to examine the quantitative differences in the BOLD response to different types of food pictures between insulin-sensitive and insulin-resistant groups. This was achieved by subtracting BOLD responses in the two groups under water and glucose challenge conditions. An additional analysis was run where BMI was included as a covariate of nuisance to control for potential confounding effects of adiposity. A second-level group-wise 2X2 repeated measures ANOVA was done (within-subject

variable: water vs. glucose; between-group variable: insulin sensitive vs. insulin resistant) to determine the effects of insulin sensitivity and condition, and their interaction on the BOLD responses to food pictures. Lastly, second-level analysis was also used to examine the potential effect of insulin sensitivity on the BOLD response to different types of food pictures across all subjects. The correlation analysis was done by combining all subjects' contrast images for a specific contrast into one group (one-sample t-test), entering the corresponding HOMA2-IR values (the covariate of interest) for each subject, and testing under water, glucose and glucose>water conditions. This analysis was repeated including BMI as a nuisance covariate.

Activation was depicted initially as a whole-brain t-map. A small volume correction (SVC) was applied to *a priori* regions of interest (ROI) to improve statistical power by enhancing sensitivity to signal changes in these regions. The corrections applied were based on previous reports showing activation in areas involved in homeostatic and hedonic control of appetite. ROIs were specified using the WFU PickAtlas toolbox in SPM8 (Maldjian *et al.*, 2003), and included the DLPFC, mPFC and anterior cingulate because they have been implicated in cognitive control. The OFC, insula, amygdala/hippocampus and basal ganglia (including caudate/putamen), substantia nigra, VTA, NAc, and fusiform were included because of their role in reward processing and because they are highly interconnected. Lastly, the hypothalamus and midbrain were included because of their role in homeostatic control of appetite as reviewed in (Van Vugt, 2010). All ROIs except the VTA and NAc were pre-defined within WFU PickAtlas; the VTA (0, -16, -10) and NAc (-10, 0, -10) masks were generated by creating a sphere with a radius of 5mm around these specific coordinates reported for these regions in previous studies (Beaver *et al.*, 2006;

Stoeckel *et al.*, 2008). The DLPFC was specified by combining the middle and superior frontal gyri selections in the WFU PickAtlas toolbox. A threshold of $p<0.001$ (uncorrected; ≥5 contiguous voxels) was first applied to the whole brain, followed by the SVC utility in SPM8 to determine if specific ROIs were activated. ROIs were considered to be significantly activated if the peak voxel met the threshold of $p < 0.05$ (corrected; ≥5 contiguous voxels). Due to the small size of the hypothalamus and VTA regions, a cluster of ≤5 contiguous voxels with a threshold of $p < 0.05$ corrected was considered significant. In the NAc, a cluster of ≤5 contiguous voxels with a threshold of $p < 0.05$ corrected was also considered significant, as in previous studies.

2.3 Demographic and behavioral data analysis

2.3.1 Demographic data

Group comparison of clinical and biochemical measurements were analyzed by two-tailed t-tests using GraphPad InStat version 3.06 (La Jolla, CA).

2.3.2 Hunger scores

Means, standard deviations (SD) and range of the pre- and post-scan hunger scores were calculated for insulin-sensitive and insulin-resistant groups, and for all subjects pooled together under control and glucose conditions. Comparison of pre- and post-scan hunger scores were analyzed by Friedman test followed by Dunn's multiple comparisons test for within-group comparisons to determine the effect of viewing food pictures on hunger. The difference between post-scan hunger scores after water and after glucose challenge conditions was also analyzed by Friedman test followed by Dunn's multiple comparisons test to determine the effect of scan conditions on hunger. Between-group

comparisons of pre- and post-scan hunger scores under both conditions were analyzed by Kruskal-Wallis test to determine the effect of insulin sensitivity on hunger.

2.3.3 Recall test

The mean, SD and range of the correct recall scores for HC, LC and C images were calculated for the insulin-sensitive and insulin-resistant groups, as well as for all subjects pooled together under control and glucose conditions. Comparisons between the mean correct recall scores of the HC, LC and C images within each group under both conditions were analyzed using Tukey's test to determine the effect of picture type on recall. The mean correct recall scores were also compared within each group for each image type using Tukey's test to determine the effect of the condition on recall.

2.3.4 PANAS

After each scan, subjects indicated on a scale of 1 to 5 how well the various descriptors (ten positive and ten negative words) on the PANAS applied to them in the past 24 hours. The total rating for the negative words (minimum score of 10, maximum score of 50) generated a negative affect score; the total rating for the positive words (minimum score of 10, maximum score of 50) generated a positive affect score. Mean, SD and range of the positive affect and negative affect scores were calculated for each group under both control and glucose conditions. Comparison of mean negative and positive affect scores between water and glucose and between insulin-sensitive and insulin-resistant groups were analyzed by Kruskal-Wallis test to determine whether condition or sensitivity affected the mood at the time of the scan. All behavioral data were statistically analyzed using GraphPad InStat version 3.06. (La Jolla, CA).

Chapter 3

Results

3.1 Demographics

Eleven of the 19 subjects were deemed to be insulin resistant based on having a HOMA2-IR≥1.7. Based on BMI, 2 subjects (both insulin sensitive) were normal weight (range: 23.5-24.2 kg/m^2), 4 subjects (3 insulin sensitive) were overweight (range: 25.8-29.7 kg/m^2), 7 subjects (2 insulin sensitive) were obese (range: 30.7-39.7 kg/m^2), and 6 subjects (1 insulin sensitive) were morbidly obese (range: 42.6-55.5 kg/m^2). BMI, WC, HOMA2-IR, and fasting insulin were significantly different between the insulin-resistant and insulin-sensitive groups, whereas age, fasting glucose, and testosterone did not differ between the two groups (Table 1). Two subjects in the insulin-resistant group were taking an insulin-sensitizing agent, metformin, and one subject in the insulin-sensitive group was taking an oral contraceptive pill at the time of the study.

3.2 Behavioral results

Mean hunger scores for the pre- and post-scan were not significantly different between the insulin-sensitive and insulin-resistant groups under either water or glucose challenge conditions (Table 2). After water consumption, the post-scan hunger score of the two groups combined was significantly increased compared to the pre-scan hunger score. Conversely, there were no differences between pre- and post-scan scores for the insulin-sensitive and insulin-resistant groups. After glucose consumption, the post-scan hunger score for all subjects, insulin-sensitive, and insulin-resistant groups did not differ significantly from their respective pre-scan hunger scores. The post-scan hunger scores

Table 1 Clinical and biochemical features of study subjects

	All subjects (n=19)	Sensitive (n=8)	Resistant (n=11)	*p
Age (years)	27.6±5.24 (18.0–39.0)	27.3±4.65 (21.0–36.0)	27.9±5.84 (18.0–39.0)	0.788
BMI (kg/m^2)	36.1±9.16 (23.5–55.5)	30.8±7.03 (23.5–42.6)	40.0±8.78 (26.7–55.5)	0.021*
WC (inches)	41.6±7.8 (32.0–60.0)	36.9±5.32 (32.0–48.0)	45.0±7.71 (34.5–60.0)	0.015*
HOMA2-IR	1.7±0.80 (0.5–3.4)	0.9±0.25 (0.5–1.2)	2.3±0.44 (1.9–3.4)	1.36E-07*
Fasting glucose (mg/dl)	89.8±9.72 (70.3–106.3)	86.0±12.90 (70.3–106.3)	92.2±6.64 (77.5–97.3)	0.270
Fasting insulin (µU/ml)	12.9±6.51 (3.5–26.6)	6.6±1.99 (3.5–9.1)	17.8±3.61 (14.5–26.6)	6.82E-07*
Testosterone (nmol/L)	2.3±0.85 (1.0–4.0)	2.4±0.91 (1.2–3.6)	2.2±0.86 (1.0–4.0)	0.678

*p value < 0.05 statistically significant for sensitive vs. resistant; two-tailed t-test.

Table 2 Effect of condition, food picture exposure and insulin sensitivity on hunger

	All subjects (n=19)	Sensitive (n=8)	Resistant (n=11)	*p
Water condition				
Pre-scan	6.5± 2.27 (2.0–10.0)	7.0±1.93 (3.0–9.0)	6.2±2.52 (2.0–10.0)	NS
Post-scan	8.1± 1.63† (5.0–10.0)	8.1± 2.10 (5.0–10.0)	8.1±1.30 (6.0–10.0)	NS
Glucose condition				
Pre-scan	6.7± 2.31 (1.0–10.0)	6.8±2.19 (4.0–10.0)	6.7±2.49 (1.0–9.0)	NS
Post-scan	7.4±1.68 (4.0–10.0)	7.4±1.85 (4.0–10.0)	7.5±1.64 (5.0–10.0)	NS

*p value > 0.05 not statistically significant (NS) for sensitive vs. resistant (in pre-scan or post-scan hunger scores); Kruskal-Wallis Test.
†p value < 0.05 statistically significant for all subjects (in pre vs. post-scan hunger score) under water condition; Friedman Test followed by Dunn's multiple comparisons test.

were not affected by treatment: in all subjects, insulin-sensitive, and insulin-resistant groups, post-scan scores after water were not significantly different from post-scan mean hunger score after the glucose challenge.

The recall scores for HC, LC and C images did not differ between insulin-sensitive and insulin-resistant subjects under water control or glucose challenge conditions (Table 3). Likewise, the recall scores for the HC, LC and C images did not differ between water and glucose challenge conditions in all subjects, insulin-sensitive, and insulin-resistant groups. Finally, there were no significant differences for both positive and negative affect (PANAS) scores between insulin-sensitive and insulin-resistant groups under water or glucose challenge conditions (Table 4). Moreover, there were no significant differences for both positive and negative affect scores between water and glucose challenge conditions in all subjects, insulin-sensitive, and insulin-resistant groups.

3.3 BOLD responses to food pictures in insulin-sensitive and insulin-resistant groups

3.3.1 Regional activation by food pictures during water condition

HC food pictures activated the insula in the insulin-sensitive group. In contrast, the HC stimulus activated the midbrain, putamen, pallidum, hippocampus, amygdala, substantia nigra, VTA, and NAc in the insulin-resistant group (Table 5). The LC stimulus activated the same regions, as well as the caudate and lentiform nucleus, in the insulin-resistant group (Table 5).

3.3.2 Regional activation by food pictures during a glucose challenge

No ROIs were activated by food pictures during a glucose challenge in the insulin-sensitive group. The BOLD signal in the DLPFC was inhibited in response to HC pictures

Table 3 Effect of type of food pictures and condition on recall test

	All subjects (n=16)	Sensitive (n=7)	Resistant (n=9)	*p
Water condition				
Control pictures	6.4± 1.46 (4.0–8.0)	6.4±1.81 (4.0–8.0)	6.4±1.24 (4.0–8.0)	NS
High-calorie pictures	5.9± 1.57 (3.0–8.0)	5.6± 1.40 (3.0–7.0)	6.2±1.72 (4.0–8.0)	NS
Low-calorie pictures	5.4±1.46 (2.0–8.0)	5.4±2.15 (2.0–8.0)	5.4±0.73 (5.0–7.0)	NS
Glucose condition				
Control pictures	6.8± 1.00 (4.0–8.0)	6.4±1.40 (4.0–8.0)	7.0±0.50 (6.0–8.0)	NS
High-calorie pictures	6.1±1.09 (4.0–8.0)	6.4±0.98 (5.0–8.0)	5.9±1.17 (4.0–7.0)	NS
Low-calorie pictures	5.6±1.37 (3.0–7.0)	5.3±1.70 (3.0–7.0)	5.8±1.09 (4.0–7.0)	NS

*p value > 0.05 not statistically significant (NS).

Table 4 Effect of insulin sensitivity and condition on PANAS

	All subjects (n=19)	Sensitive (n=8)	Resistant (n=11)	*p
Water condition				
Positive Affect-score	35±7.1 (23–47)	37.0±6.4 (25–43)	33.5±7.5 (23–47)	NS
Negative Affect-score	15.9±4.4 (10–24)	14.5±3.6 (10–20)	17.0±4.7 (10–24)	NS
Glucose condition				
Positive Affect-score	31.6±9.0 (14–49)	32.9±10.2 (18–49)	30.7±8.5 (14–39)	NS
Negative Affect-score	16.7±7.7 (10–36)	13.9±3.8 (10–20)	18.7±9.2 (10–36)	NS

*p value > 0.05 not statistically significant (NS).

Table 5 Differential BOLD response to food pictures during water condition in insulin-sensitive and insulin-resistant groups

		Water		
Region	**Hem**	**Cluster (K)**	**t stat**	**MNI coordinates (x y z)**
Insulin-Sensitive				
HC-C				
DLPFC	L	15	8.59	(-22 26 -18)
	R	12	7.19	(24 30 -12)
OFC	L	21	8.59	(-22 26 -18)
	R	27	7.63	(26 30 -14)
Insula	**L**	**79**	**11.39**	**(-38 -4 -4)**
	R	**14**	**6.4**	**(40 8 -8)**
LC-C				
DLPFC	L	9	7.65	(-54 36 10)
	R	28	7.8	(42 34 14)
Insula	L	14	6.49	(-36 -4 6)
	R	5	5.35	(38 2 18)
Hippocampus	L	7	5.52	(-30 -32 -4)
HC-LC				
DLPFC	L	10	5.99	(-32 34 36)
	R	20	6.27	(24 6 60)
Insulin-Resistant				
HC-C				
DLPFC	L	14	5.11	(-44 46 12)
	R	57	7.49	(50 14 32)
OFC	R	10	5.09	(10 36 18)
Midbrain	**L/R**	**497**	**7.79**	**(-12 -18 -8)**
			7.08	**(8 -26 -6)**
Caudate	L	6	4.38	(-10 10 -2)
	R	8	5.29	(10 6 12)
Putamen	**L**	**16**	**5.43**	**(-32 0 -4)**
	R	**57**	**6.39**	**(34 -4 4)**
Pallidum	**L**	**9**	**4.79**	**(-24 -14 2)**

	R	**26**	**5.93**	**(28 -12 -2)**
Lentiform Nucleus	L	44	5.42	(-24 -16 2)
	R	84	5.93	(28 -12 -2)
Anterior Cingulate	R	10	5.09	(10 36 18)
Insula	L	7	4.61	(-38 -4 4)
	R	20	5.3	(38 -4 4)
Hippocampus	**L**	**54**	**9.5**	**(-18 -32 -2)**
	R	**14**	**5.37**	**(26 -28 -6)**
Amygdala	**L**	**34**	**5.06**	**(-26 -8 -14)**
	R	**80**	**6.48**	**(28 -4 -12)**
Substantia Nigra	**L**	**14**	**5.98**	**(-8 -18 -12)**
	R	**10**	**5.29**	**(12 -16 -12)**
VTA	**L/R**	**34**	**6.97**	**(-4 -18 -12)**
			6.38	**(4 -18 -12)**
NAc	**R**	**4**	**4.53**	**(10 -4 -8)**
LC-C				
DLPFC	L	16	6.95	(-40 40 14)
	R	20	5.97	(50 12 30)
mPFC	L	29	6.55	(-6 24 38)
Midbrain	**L/R**	**184**	**6.5**	**(-6 -30 -20)**
			9.01	**(6 -18 -12)**
Caudate	**L**	**10**	**5.53**	**(-12 12 -2)**
	R	**37**	**7.52**	**(14 14 -6)**
Putamen	**L**	**39**	**6**	**(-14 10 -4)**
	R	**43**	**7.6**	**(14 12 -6)**
Pallidum	**L**	**6**	**4.84**	**(-16 8 -2)**
	R	**20**	**7.5**	**(22 -6 -2)**
Lentiform Nucleus	**L**	**42**	**7.13**	**(-16 8 -12)**
	R	**56**	**8.1**	**(18 -10 -2)**
Insula	L	35	5.88	(-38 -4 4)
	R	52	5.96	(40 -2 4)
Hippocampus	**L**	**35**	**6.78**	**(-30 -10 -12)**
	R	**34**	**6.6**	**(24 -32 -2)**
Amygdala	**L**	**32**	**6.11**	**(-28 -8 -12)**
	R	**19**	**4.87**	**(28 0 -14)**
Substantia Nigra	**L**	**1**	**4.23**	**(-10 -16 -10)**
	R	**4**	**6.06**	**(10 -20 -12)**
NAc	**R**	**5**	**5.33**	**(12 -4 -12)**
VTA	**R**	**10**	**6.3**	**(4 -18 -12)**

HC-LC				
DLPFC	L	20	6.01	(-26 36 -6)
OFC	L	20	5.48	(-22 36 -10)

Regions with significant activation by high-calorie (HC) or low-calorie food pictures (LC) vs. control pictures (C), or by HC vs. LC, at a threshold of $p < 0.001$ (uncorrected) with a minimum cluster size of 5 voxels (except for NAc and substantia nigra where a minimum of one voxel was considered significant). The regions satisfying the family-wise error (FWE) threshold of $p < 0.05$ (corrected) are highlighted in bold. Abbreviations: left (L), right (R), hemisphere (hem), number of voxels in a cluster (k), Montreal Neurological Institute (MNI), dorsolateral prefrontal cortex (DLPFC), orbitofrontal cortex (OFC), medial prefrontal cortex (mPFC), nucleus accumbens (NAc), and ventral tegmental area (VTA).

in the insulin-sensitive group (Table 6). In contrast, many regions were activated by food cues during a glucose challenge in the insulin-resistant group (Table 6). In the insulin-resistant group, HC pictures activated the DLPFC, OFC, midbrain, caudate, putamen, pallidum, lentiform nucleus, insula, hippocampus, amygdala, substantia nigra, VTA and fusiform, and LC pictures activated the same regions (except the DLPFC), and the NAc (Table 6). Statistical parametric maps showing comparisons of brain responses to food pictures in some of the ROIs in insulin-sensitive and insulin-resistant groups during a glucose challenge are shown in (Figure 5 and 6).

3.3.3 Effects of water vs. glucose condition on brain activation by food pictures

Both the insulin-sensitive and insulin-resistant groups exhibited greater activation in several (but different) ROIs during the water condition than the glucose condition (water vs. glucose) (Table 7). In the insulin-sensitive group, this differential response was observed to HC pictures in the OFC, NAc, hypothalamus, and fusiform, whereas LC pictures differentially activated the insula. The DLPFC, brainstem, and hippocampus of the insulin-sensitive group were differentially activated by the HC-LC contrast (Table 7). Conversely, in the insulin-resistant group, the differential response (water vs. glucose) was observed in the midbrain to HC pictures and in the DLPFC, mPFC, VTA, and NAc to HC vs. LC pictures (Table 7). Regions that met the family-wise error (FWE) threshold are indicated in bold (Table 7).

3.4 Group differences in BOLD responses to food pictures

3.4.1 Insulin-sensitive vs. insulin-resistant subjects during water condition

The DLPFC was activated in the insulin-sensitive group compared to the insulin-resistant group for the HC-LC contrast. Inclusion of BMI as a covariate of nuisance

Table 6 Differential BOLD response to food pictures during a glucose challenge in insulin-sensitive and insulin-resistant groups

		Glucose		
Region	**Hem**	**Cluster (K)**	**t stat**	**MNI coordinates (x y z)**
Insulin-Sensitive				
HC-C				
DLPFC	L	8	6.18	(-32 50 28)
Negative				
DLPFC	**L**	**82**	**-12.61**	**(-28 28 42)**
	R	**90**	**-7.93**	**(28 38 40)**
mPFC	L	5	-5	(-4 42 22)
	R	11	-6.02	(4 58 28)
Anterior Cingulate	L/R	49	-5.22	(-2 42 20)
			-7.89	(6 42 20)
Insula	L	5	-5.34	(-40 -24 18)
LC-C				
DLPFC	R	25	7.2	(44 34 14)
Insula	L	29	5.87	(-42 -4 -4)
Negative				
DLPFC	L	38	-8.94	(-30 28 40)
	R	11	-6.04	(34 30 38)
mPFC	L	10	-7.7	(-8 42 44)
Insula	R	5	-7.98	(58 -36 18)
HC-LC				
Negative				
DLPFC	L	16	-9.1	(-30 34 -14)
Insulin-Resistant				
HC-C				
DLPFC	**L**	**62**	**8.86**	**(-30 34 -16)**
	R	**17**	**5.91**	**(48 12 30)**
mPFC	L	16	5.31	(-6 26 38)
OFC	**L**	**106**	**8.86**	**(-30 34 -16)**
	R	**28**	**5.63**	**(32 32 -10)**

Midbrain	**L**	**56**	**6.9**	**(-18 -26 -6)**
	R	**25**	**6.27**	**(12 -10 -2)**
Anterior Cingulate	R	6	6.09	(4 2 28)
Caudate	**L**	**6**	**5.12**	**(-12 -8 16)**
	R	**83**	**7.71**	**(10 12 6)**
Putamen	**L**	**45**	**6.2**	**(-24 10 -4)**
	R	**61**	**13.59**	**(36 0 -2)**
Pallidum	**L**	**24**	**6.49**	**(-26 -6 -2)**
	R	**12**	**5.07**	**(14 8 0)**
Lentiform Nucleus	**L**	**38**	**6.49**	**(-26 -6 -2)**
	R	**50**	**5.41**	**(18 12 6)**
Insula	**L**	**245**	**10.86**	**(-36 12 -12)**
	R	**215**	**18.38**	**(36 2 -2)**
Hippocampus	**L**	**11**	**7.75**	**(-34 -14 -12)**
	R	**29**	**8.16**	**(20 -34 2)**
Amygdala	**L**	**62**	**11.42**	**(-28 2 -16)**
	R	**64**	**7.29**	**(28 2 -14)**
Substantia Nigra	**L**	**5**	**5.91**	**(-6 -14 -10)**
VTA	**L**	**4**	**6.52**	**(-4 -18 -10)**
Fusiform	**L**	**811**	**14.06**	**(-38 -58 -18)**
	R	**821**	**20.46**	**(40 -56 -16)**
Negative				
DLPFC	L	8	-4.83	(-26 34 36)
	R	65	-5.97	(26 34 42)
Insula	L	23	-6.92	(-48 -26 20)
LC-C				
DLPFC	L	17	7.28	(-42 2 38)
	R	54	7.37	(48 38 18)
mPFC	L	17	6.6	(-6 52 42)
	R	6	5.23	(12 32 42)
OFC	**L**	**50**	**6.53**	**(-24 32 -18)**
	R	**40**	**8.09**	**(38 26 -10)**
Midbrain	**L**	**14**	**7.47**	**(-20 -30 -4)**
	R	**5**	**5.59**	**(20 -30 -4)**
Caudate	**L**	**69**	**7.39**	**(-8 12 2)**
	R	**271**	**14.61**	**(12 12 6)**
Putamen	**L**	**31**	**5.49**	**(-22 2 -10)**
	R	**94**	**14.63**	**(34 -2 -2)**
Pallidum	**L**	**29**	**5.87**	**(-12 -2 0)**
	R	**14**	**5.28**	**(20 -2 6)**
Lentiform Nucleus	**L**	**115**	**6.34**	**(-16 -4 6)**
	R	**69**	**6.21**	**(20 2 12)**
Insula	**L**	**130**	**5.99**	**(-38 8 -14)**
	R	**217**	**13.31**	**(36 0 -2)**

Hippocampus	**L**	**54**	**9.94**	**(-20 -30 -8)**
	R	**38**	**7.22**	**(20 -32 -2)**
Amygdala	**L**	**50**	**7.61**	**(-24 0 -20)**
	R	**57**	**7.18**	**(26 -4 -12)**
Substantia Nigra	**L**	**3**	**5.01**	**(-6 -12 -12)**
VTA	**L**	**7**	**6.25**	**(-4 -14 -12)**
NAc	**R**	**9**	**5.78**	**(12 -2 -6)**
Fusiform	**L**	**552**	**7.07**	**(-30 -80 -18)**
	R	**656**	**9.23**	**(26 -46 -18)**
HC-LC				
Negative				
DLPFC	L	21	-5.06	(-40 32 20)
	R	8	-4.89	(24 36 36)
Putamen	R	16	-5.42	(30 -4 8)

Regions with significant activation by high-calorie (HC) or low-calorie food pictures (LC) vs. control pictures (C), or by HC vs. LC, at a threshold of $p < 0.001$ (uncorrected) with a minimum cluster size of 5 voxels (except for VTA and substantia nigra where a minimum of one voxel was considered significant). The regions satisfying the family-wise error (FWE) threshold of $p < 0.05$ (corrected) are highlighted in bold. The t stat with a minus (-) sign means a negative activation in the region of interest. Abbreviations: left (L), right (R), hemisphere (hem), number of voxels in a cluster (k), Montreal Neurological Institute (MNI), dorsolateral prefrontal cortex (DLPFC), orbitofrontal cortex (OFC), medial prefrontal cortex (mPFC), nucleus accumbens (NAc), and ventral tegmental area (VTA).

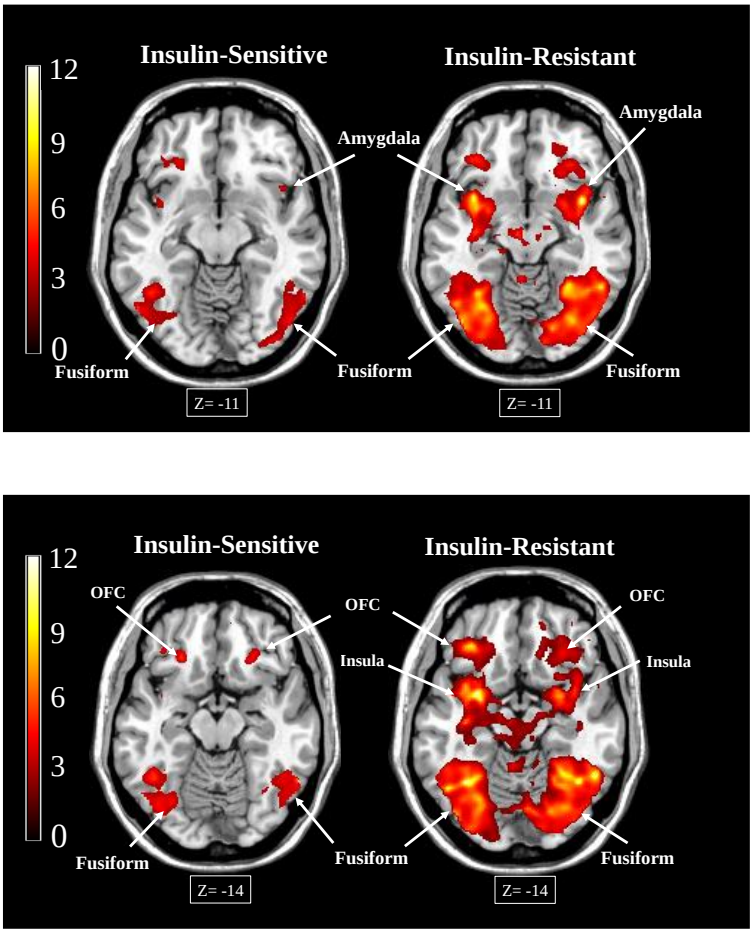

Figure 5: BOLD response in the amygdala, fusiform, OFC and insula in insulin-sensitive and insulin-resistant subjects during a glucose challenge

Statistical parametric maps showing activation in response to food compared to control (C) pictures were generated for the whole brain after BMI was included as a covariate of nuisance. Activation is depicted in slice overlays onto the MRI croN single subject T1 template. The MNI Z coordinates for the axial planes are indicated in each map. An uncorrected threshold of $P < 0.001$ was used for display purposes. The t value of functional activity is indicated by the color scale. Activation in response to Food – C following glucose ingestion was increased in the insulin-resistant group (n=11) compared to the insulin-sensitive group (n=8) in the amygdala and fusiform (top panel), orbitofrontal cortex (OFC), insula and fusiform (bottom B). Only ROIs are labeled.

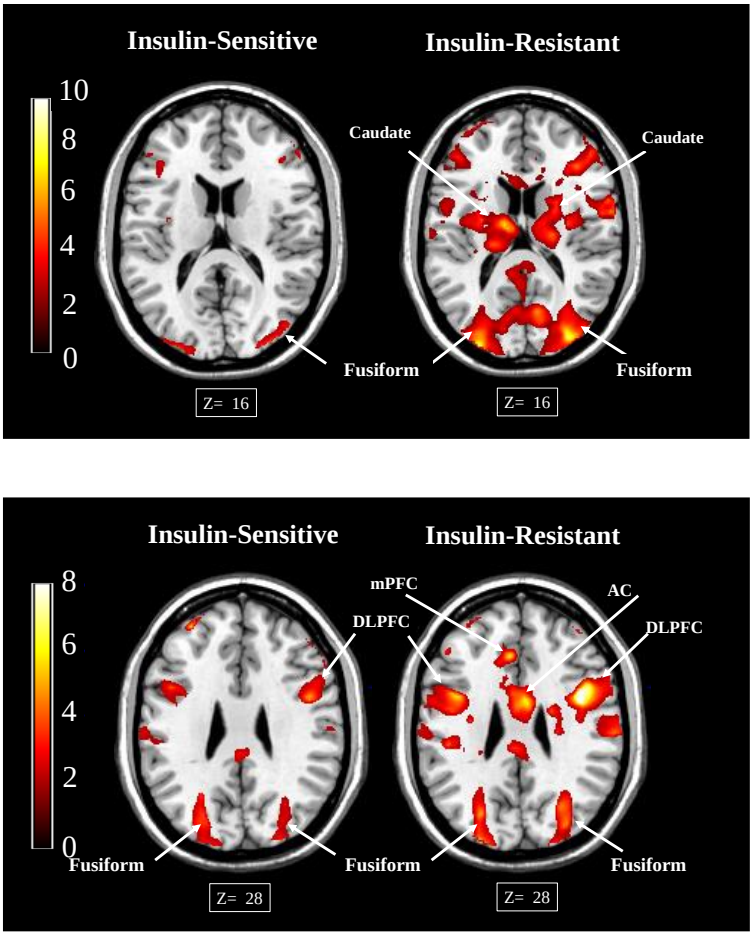

Figure 6: BOLD response in the caudate, fusiform, mPFC, AC, and DLPFC in insulin-sensitive and insulin-resistant subjects during a glucose challenge

Statistical parametric maps showing activation in response to food compared to control (C) pictures were generated for the whole brain after BMI was included as a covariate of nuisance. Activation is depicted in slice overlays onto the MRI croN single subject T1 template. The MNI Z coordinates for the axial planes are indicated in each map. An uncorrected threshold of $P < 0.001$ was used for display purposes. The t value of functional activity is indicated by the color scale. Activation in response to Food – C following glucose ingestion was increased in the insulin-resistant group (n=11) compared to the insulin-sensitive group (n=8) in the caudate and fusiform (top panel), medial prefrontal cortex (mPFC), anterior cingulate (AC), dorsolateral prefrontal cortex (DLPFC) and fusiform (bottom panel). Only ROIs are labeled.

Table 7 Differential BOLD response to food pictures after water vs. glucose condition in insulin-sensitive and insulin-resistant groups

		Water > Glucose		
Region	**Hem**	**Cluster (K)**	**t stat**	**MNI coordinates (x y z)**
Insulin-Sensitive				
HC-C				
OFC	R	6	7.56	(10 40 -14)
NAc	**L**	**2**	**5.93**	**(-6 -2 -12)**
Hypothalamus	**L**	**1**	**6.8**	**(-4 -2 -12)**
Fusiform	R	5	6.78	(36 -36 -24)
LC-C				
Insula	R	8	7.81	(38 0 16)
HC-LC				
DLPFC	R	9	8.66	(32 48 6)
Brainstem	R	13	7.69	(10 -28 -36)
Hippocampus	R	23	6.9	(30 -22 -14)
Insulin-Resistant				
HC-C				
Midbrain	L	12	5.28	(-8 -24 -16)
HC-LC				
DLPFC	L	34	5.72	(-38 20 42)
	R	22	5.9	(12 58 26)
mPFC	L	7	4.39	(-2 46 36)
	R	15	5.9	(12 58 26)
VTA	**L**	**2**	**4.53**	**(-2 -18 -6)**
NAc	**L**	**3**	**4.79**	**(-10 4 -8)**

Regions with significant activation by high-calorie (HC) or low-calorie food pictures (LC) vs. control pictures (C), or by HC vs. LC, at a threshold of $p < 0.001$ (uncorrected) with a minimum cluster size of 5 voxels (except for VTA, NAc and hypothalamus where a minimum of one voxel was considered significant). The regions satisfying the family-wise error (FWE) threshold of $p < 0.05$ (corrected) are highlighted in bold. Contrasts lacking significant effects are not shown. Abbreviations: left (L), right (R), hemisphere (hem), number of voxels in a cluster (k), Montreal Neurological Institute (MNI), dorsolateral prefrontal cortex (DLPFC), orbitofrontal cortex (OFC), medial prefrontal cortex (mPFC), nucleus accumbens (NAc), and ventral tegmental area (VTA).

eliminated the DLPFC activation on the right side (R) and uncovered activation on the left side (L) (Table 8). In contrast, the LC pictures increased the BOLD response in the DLPFC in the insulin-resistant vs. the insulin-sensitive groups only when BMI was added as a nuisance covariate (Table 8).

3.4.2 Insulin-sensitive vs. insulin-resistant subjects during a glucose challenge

The BOLD response to both HC and LC pictures during the glucose challenge was increased in the insulin-resistant compared to the insulin-sensitive group in the DLPFC, mPFC, caudate and insula. The BOLD response in the brainstem and anterior cingulate was increased in response to HC pictures in the insulin-resistant compared to the insulin-sensitive group following the glucose challenge (Table 9). In contrast, the BOLD response in the DLPFC, pallidum, and lentiform nucleus was increased in the insulin-sensitive compared to the insulin-resistant group to the HC-LC contrast (Table 9). Many of the regions described above also met the FWE threshold (see Table 9).

When BMI was included as a nuisance covariate, the significance level of the BOLD signal to HC pictures was increased in the DLPFC, mPFC, anterior cingulate, and insula. However, the significance level of the BOLD signal was reduced in the brainstem and eliminated in the caudate. This analysis also revealed additional significant activation in the putamen in the insulin-resistant compared to the insulin-sensitive group. Including BMI as a covariate of nuisance reduced the significance level of the BOLD signal to LC pictures in the DLPFC and mPFC, maintained the significance level in the caudate, revealed additional significant activation in the pallidum and anterior cingulate, and increased the significance level of the BOLD signal in the insula of the insulin-resistant compared to insulin-sensitive group. This analysis also revealed an increase in the BOLD signal in the

Table 8 Group differences in the BOLD response to food pictures during water condition

		Water						
		Without BMI				With BMI		
				Sensitive > Resistant				
Region	**Hem**	**Cluster (K)**	**t stat**	**MNI coordinates (x y z)**	**Hem**	**Cluster (K)**	**t stat**	**MNI coordinates (x y z)**
HC-LC								
DLPFC	R	16	4.37	(34 6 62)	L	29	5.33	(-20 12 66)
				Resistant > Sensitive				
LC-C								
DLPFC					L	8	4.11	(-20 54 16)
					R	16	4.78	(32 22 52)

Regions with significant activation by high-calorie (HC) or low-calorie food pictures (LC) vs. control pictures (C), or by HC vs. LC, at a threshold of $p < 0.001$ (uncorrected) with a minimum cluster size of 5 voxels. Contrasts lacking significant effects are not shown. Abbreviations: left (L), right (R), hemisphere (hem), number of voxels in a cluster (k), Montreal Neurological Institute (MNI), body mass index (BMI), and dorsolateral prefrontal cortex (DLPFC).

Table 9 Group differences in the BOLD response to food pictures during a glucose challenge

				Glucose				
		Without BMI				**With BMI**		
				Resistant>Sensitive				
Region	**Hem**	**Cluster (K)**	**t stat**	**MNI coordinates (x y z)**	**Hem**	**Cluster (K)**	**t stat**	**MNI coordinates (x y z)**
HC-C								
DLPFC	L	38	6.13	(-12 20 62)	**L**	**46**	**7.16**	**(-12 20 62)**
					R	**10**	**5.49**	**(32 4 42)**
mPFC	L	7	4.28	(-8 40 26)	**L**	**13**	**4.48**	**(-2 42 24)**
					R	**26**	**5.85**	**(12 30 46)**
Brainstem	**L**	**28**	**5.4**	**(-10 -28 -26)**	L	18	4.62	(-12 -28 -26)
Caudate	R	9	4.11	(8 12 6)				
Putamen					**L**	**11**	**4.88**	**(-30 -2 8)**
Anterior Cingulate	R	15	4.53	(10 40 20)	**L**	**89**	**3.86**	**(-4 16 28)**
					R		**4.99**	**(4 20 24)**
Insula	R	7	5.19	(40 14 10)	**L**	**20**	**4.5**	**(-34 -30 14)**
					R	**11**	**6.21**	**(38 -14 -8)**
LC-C								
DLPFC	**L**	**32**	**6.38**	**(-30 26 44)**	L	19	5.63	(-30 26 44)
					R	131	6.27	(20 48 24)
mPFC	**L**	**39**	**5.82**	**(-8 44 46)**	L	17	5.22	(-8 44 46)
	R	**18**	**4.84**	**(10 34 42)**	R	16	4.98	(12 44 32)
Caudate	**R**	**35**	**5.34**	**(10 12 4)**	**R**	**16**	**4.7**	**(10 12 2)**
Pallidum					**R**	**7**	**4.48**	**(22 -6 -4)**
Anterior Cingulate					R	37	4.61	(8 32 20)
Insula	L	9	4.75	(-26 12 -18)	**R**	**27**	**5.6**	**(40 12 12)**

	R	7	4.21	(38 12 12)				
HC-LC								
DLPFC					R	5	4.29	(34 46 34)
Fusiform					L	33	4.86	(-26 -72 -6)
				Sensitive > Resistant				
HC-LC								
DLPFC	L	8	4.22	(-50 28 24)				
Pallidum	**R**	**8**	**4.39**	**(22 -4 -4)**				
Lentiform Nucleus	R	8	4.39	(22 -4 -4)				

Regions with significant activation by high-calorie (HC) or low-calorie food pictures (LC) vs. control pictures (C), or by HC vs. LC, at a threshold of $p < 0.001$ (uncorrected) with a minimum cluster size of 5 voxels. The regions satisfying the family-wise error (FWE) threshold of $p < 0.05$ (corrected) are highlighted in bold. Contrasts lacking significant effects are not shown. Abbreviations: left (L), right (R), hemisphere (hem), number of voxels in a cluster (k), Montreal Neurological Institute (MNI), body mass index (BMI), dorsolateral prefrontal cortex (DLPFC), and medial prefrontal cortex (mPFC).

DLPFC and fusiform to HC-LC contrast in the insulin-resistant compared to insulin-sensitive group (Table 9). Conversely, including BMI as a covariate of nuisance eliminated the significance level of the BOLD signal to HC-LC contrast in the DLPFC, pallidum, and lentiform nucleus in the insulin-sensitive compared to insulin-resistant group following the glucose challenge (Table 9). The aforementioned regions also met the FWE threshold (see Table 9).

3.5 Interaction between insulin sensitivity and study condition

There was a significant interaction between insulin sensitivity and study condition in response to food pictures. A positive interaction was seen in the insula (L) and fusiform in response to HC pictures, in the insula (R) and midbrain in response to LC pictures, and in the fusiform in response to HC vs. LC pictures (Table 10). There was a significant difference detected between the insulin-sensitive and insulin-resistant groups between conditions. BOLD response to HC pictures was bilateral in fusiform when BMI was added as a covariate of nuisance (Table 10). This analysis identified regions that exhibited greater activation during a glucose challenge compared to water in insulin-resistant subjects compared to insulin-sensitive subjects. A negative interaction analysis was conducted, but no significant effects were observed (data not shown). Regions that met the FWE threshold are highlighted in bold (Table 10). The interaction between insulin sensitivity and experimental condition on brain responsiveness to food pictures for some ROIs is illustrated in (Figure 7).

Table 10 Interaction between insulin sensitivity and condition

	Interaction							
	Without BMI				With BMI			
Region	**Hem**	**Cluster (K)**	**t stat**	**MNI coordinates (x y z)**	**Hem**	**Cluster (K)**	**t stat**	**MNI coordinates (x y z)**
Positive interaction								
HC-C								
Insula	L	7	4.01	(-32 14 16)	L	7	4.01	(-32 14 16)
Fusiform	R	12	3.94	(28 -30 -24)	L	9	3.89	(-20 -46 -14)
					R	11	3.83	(28 -42 -12)
LC-C								
Midbrain	**L**	**6**	**4.11**	**(-10 -12 -12)**	**L**	**6**	**4.01**	**(-10 -12 -12)**
Insula	R	8	4.3	(38 4 18)	R	7	4.29	(38 4 18)
HC-LC								
Fusiform	R	9	3.54	(34 -32 -22)	R	12	3.56	(34 -32 -22)

Regions with significant activation by high-calorie (HC) or low-calorie food pictures (LC) vs. control pictures (C), or by HC vs. LC, at a threshold of $p < 0.001$ (uncorrected) with a minimum cluster size of 5 voxels. The regions satisfying the family-wise error (FWE) threshold of $p < 0.05$ (corrected) are highlighted in bold. Abbreviations: left (L), right (R), hemisphere (hem), number of voxels in a cluster (k), Montreal Neurological Institute (MNI), and body mass index (BMI).

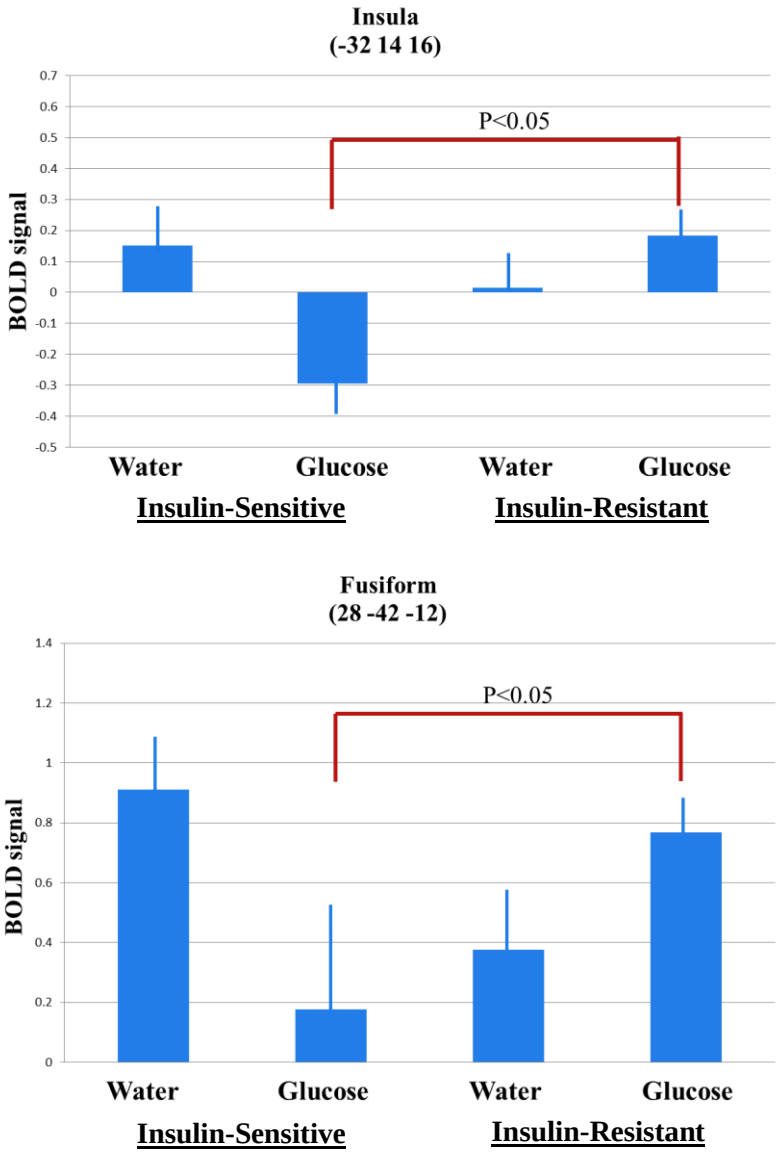

Figure 7: Interaction between insulin sensitivity and condition

BOLD signal induced by food pictures (Food – C) following water or glucose was compared in insulin-sensitive (n=8) and insulin-resistant groups (n=11) after BMI was included as a covariate of nuisance. Mean parameter estimate of BOLD effect size (±SEM) was extracted for a 5mm radius sphere centered on the peak voxel in the insula (-32 14 16) and fusiform (28 -42 -12). Significant differences between groups are indicated in the figure ($p<0.05$; ANOVA and Tukey's Post Hoc Test).

3.6 Correlation between insulin resistance and corticolimbic BOLD response to food pictures

3.6.1 Correlation between insulin resistance and BOLD response to food pictures during water condition

A positive correlation between the degree of insulin resistance (as measured by HOMA2-IR) and the BOLD signal in response to LC pictures following water consumption was seen in the hippocampus (Table 11). The BOLD signal in the DLPFC was negatively correlated with HOMA2-IR in response to HC-LC contrast (Table 11). Adding BMI as a nuisance covariate maintained the positive correlation between HOMA2-IR and the BOLD signal in the hippocampus (however, it decreased the significance of the activation detected) and revealed a positive correlation between HOMA2-IR and the BOLD signal in the DLPFC in response to LC pictures and the caudate in response to HC vs. LC pictures (Table 11). Adding BMI revealed a negative correlation between HOMA2-IR and the BOLD signal in the fusiform in response to HC pictures. The negative correlation between HOMA2-IR and the BOLD signal in the DLPFC was maintained in response to HC-LC contrast (Table 11). The above regions that met the FWE are indicated in bold (Table 11).

3.6.2 Correlation between insulin resistance and BOLD response to food pictures during a glucose challenge

HOMA2-IR values were significantly correlated with the magnitude of the activation in numerous ROIs during the glucose challenge (Table 12). HOMA2-IR values were positively correlated with the BOLD signal in the DLPFC, brainstem, caudate, anterior cingulate, insula, and VTA in response to HC pictures, and with the BOLD signal in the

Table 11 Correlation between insulin resistance and BOLD response to food pictures during water condition

				Water				
		Without BMI					**With BMI**	
				Positive correlation				
Region	**Hem**	**Cluster (K)**	**t stat**	**MNI coordinates (x y z)**	**Hem**	**Cluster (K)**	**t stat**	**MNI coordinates (x y z)**
LC-C								
Hippocampus	**L**	**16**	**4.91**	**(-28 -10 -20)**	L	14	4.4	(-26 -10 -20)
DLPFC					L	6	4.09	(-20 54 16)
HC-LC								
Caudate					R	5	4.61	(20 -24 26)
				Negative correlation				
HC-C								
Fusiform					L	9	4.19	(-36 -74 -14)
HC-LC								
DLPFC	L	5	4.14	(-20 -18 64)	L	7	5.01	(-18 14 66)
	R	22	4.62	(30 6 56)	R	5	4.11	(34 6 62)

Regions with significant activation by high-calorie (HC) or low-calorie food pictures (LC) vs. control pictures (C), or by HC vs. LC, at a threshold of $p < 0.001$ (uncorrected) with a minimum cluster size of 5 voxels. The regions satisfying the family-wise error (FWE) threshold of $p < 0.05$ (corrected) are highlighted in bold. Contrasts lacking significant effects are not shown. Abbreviations: left (L), right (R), hemisphere (hem), number of voxels in a cluster (k), Montreal Neurological Institute (MNI), body mass index (BMI), and dorsolateral prefrontal cortex (DLPFC).

Table 12 Correlation between insulin resistance and BOLD response to food pictures during a glucose challenge

				Glucose challenge				
		Without BMI				**With BMI**		
				Positive correlation				
Region	**Hem**	**Cluster (K)**	**t stat**	**MNI coordinates (x y z)**	**Hem**	**Cluster (K)**	**t stat**	**MNI coordinates (x y z)**
HC-C								
DLPFC	L	9	4.79	(-20 60 22)	L	15	4.42	(-36 52 20)
					R	26	5.9	(30 10 42)
mPFC					**R**	**12**	**5.64**	**(12 30 48)**
OFC					**L**	**6**	**3.98**	**(-2 28 -2)**
					R	**87**	**5.9**	**(10 40 18)**
Brainstem	R	10	4.67	(16 -26 -26)	L	5	4.09	(-2 -14 -10)
Caudate	L	5	3.99	(-6 10 10)	L	9	4.52	(-6 10 10)
	R	11	4.56	(6 12 6)				
Anterior Cingulate	L	7	3.97	(-10 46 10)	**R**	**104**	**5.9**	**(10 40 18)**
	R	**20**	**5.69**	**(10 40 20)**				
Insula	L	5	4.73	(-32 -10 22)	L	32	5.01	(-36 -30 18)
					R	41	5.22	(46 4 12)
VTA	**L**	**2**	**3.84**	**(-4 -14 -12)**	**L**	**5**	**4.09**	**(-2 -14 -10)**
LC-C								
DLPFC	**L**	**14**	**6.4**	**(-8 46 46)**	**L**	**140**	**6.84**	**(-16 48 32)**
					R	**192**	**7.5**	**(20 48 24)**
mPFC	**L**	**27**	**6.4**	**(-8 46 46)**	**L**	**11**	**5.29**	**(-8 46 46)**
	R	**22**	**5.23**	**(12 34 40)**	**R**	**34**	**5.55**	**(16 46 24)**
OFC					L	12	4.15	(-12 34 16)
					R	50	5.2	(8 36 12)
Caudate	**R**	**17**	**5.13**	**(8 12 4)**				

Anterior Cingulate					**R**	**15**	**5.75**	**(16 46 20)**
Insula					**R**	**23**	**5.63**	**(44 10 12)**
HC-LC								
DLPFC	R	15	4.52	(30 44 -2)	L	63	4.9	(-36 48 26)
					R	31	5.97	(30 36 -16)
OFC	L	7	4.74	(-34 32 -18)	**L**	**44**	**6.37**	**(-34 34 -18)**
					R	**39**	**5.97**	**(30 36 -16)**
Midbrain	**L**	**7**	3.64	(-2 -30 0)	**R**	**11**	**8.61**	**(4 -32 0)**
	R		**3.96**	**(4 -32 0)**				
Hippocampus					**L**	**22**	**5.11**	**(-16 -8 -18)**
Amygdala					**L**	**37**	**5.21**	**(-28 2 -22)**
					R	**6**	**4.48**	**(24 0 -20)**
Fusiform					L	9	4.35	(-24 -72 -6)
				Negative correlation				
LC-C								
DLPFC					R	8	3.94	(38 58 2)
HC-LC								
DLPFC	**L**	**59**	**5.86**	**(-48 28 22)**	L	13	4.74	(-48 28 22)
	R	**65**	**5.82**	**(44 28 30)**				
Putamen	R	8	4.06	(32 -8 6)				

Regions with significant activation by high-calorie (HC) or low-calorie food pictures (LC) vs. control pictures (C), or by HC vs. LC, at a threshold of $p < 0.001$ (uncorrected) with a minimum cluster size of 5 voxels (except for VTA a minimum of one voxel is considered significant). The regions satisfying the family-wise error (FWE) threshold of $p < 0.05$ (corrected) are highlighted in bold. Contrasts lacking significant effects are not shown. Abbreviations: left (L), right (R), hemisphere (hem), number of voxels in a cluster (k), Montreal Neurological Institute (MNI), body mass index (BMI), dorsolateral prefrontal cortex (DLPFC), medial prefrontal cortex (mPFC), orbitofrontal cortex (OFC) and ventral tegmental area (VTA).

DLPFC, mPFC, and caudate in response to LC pictures. A positive correlation was also found between HOMA2-IR and the BOLD signal in the DLPFC, OFC and midbrain by HC vs. LC pictures (Table 12). A negative correlation was found between HOMA2-IR values and the BOLD signal in the DLPFC and putamen in response to HC vs. LC pictures (Table 12). Those regions that met the FWE threshold are indicated in bold (Table 12).

Including BMI as a covariate of nuisance maintained the positive correlation between HOMA2-IR values and the BOLD signal in the DLPFC, brainstem, caudate, anterior cingulate, insula, and VTA in response to HC pictures. Following the addition of BMI as a nuisance covariate, the correlation in the DLPFC was bilateral and had a larger cluster size; anterior cingulate and VTA also had a larger cluster size (Table 12). This analysis also revealed additional positive correlations between HOMA2-IR values and the BOLD signal in the mPFC and OFC by HC pictures. A positive correlation between HOMA2-IR and BOLD signal was maintained after adding BMI as a nuisance covariate in the DLPFC and mPFC in response to LC, which showed bilateral activation and had larger cluster sizes (Table 12). This analysis uncovered additional positive correlations between HOMA2-IR and the BOLD signal in the OFC, anterior cingulate and insula, and eliminated the correlation in the caudate in response to LC pictures (Table 12). Moreover, including BMI as a nuisance covariate showed that HOMA2-IR values positively correlated with the BOLD signal in the DLPFC, OFC and midbrain (all regions had a larger cluster size) and uncovered additional positive correlations between the HOMA2-IR and the BOLD signal in the hippocampus, amygdala and fusiform by exposure to HC vs. LC pictures (Table 12).

The relationship between insulin resistance and brain responses to food pictures was further characterized by extracting the parameter estimate of the peak voxel for the various

ROIs and performing a regression analysis between this estimate of effect size and the HOMA2-IR. Certain regions that showed a significant correlation between activity and insulin resistance during a glucose challenge are shown in (Figure 8 and 9). Including BMI as a covariate of nuisance revealed a negative correlation between HOMA2-IR values and the BOLD signal in the DLPFC in response to LC pictures, decreased the significance of the activation in the DLPFC in response to HC vs. LC pictures and eliminated the correlation seen in the putamen in response to HC vs. LC pictures (Table 12). Almost all regions indicated above met the FWE threshold (see Table 12).

3.6.3 Correlation between insulin resistance and BOLD response to food pictures during glucose vs. water condition

The magnitude of the differential activation (glucose>water) in the DLPFC, midbrain, insula and fusiform correlated with HOMA2-IR values and in response to HC pictures, and in the DLPFC, OFC, midbrain, and fusiform in response to HC vs. LC pictures (Table 13). Including BMI as a covariate of nuisance revealed further positive correlations between HOMA2-IR and the differential activation in the bilateral DLPFC and mPFC, but eliminated the correlation seen in the midbrain, insula and fusiform in response to HC pictures. This analysis uncovered a positive correlation in the midbrain in response to LC pictures (Table 13). Finally, adding BMI as a nuisance covariate maintained the positive correlation between HOMA2-IR and the differential activation in the DLPFC, midbrain and fusiform, with the DLPFC and fusiform showing bilateral activation and larger cluster size, and revealed positive correlations in the hippocampus and amygdala. Conversely, it eliminated the positive correlation in the OFC in response to HC vs. LC pictures (Table 13). Regions that met the FWE threshold are indicated in bold (see Table 13).

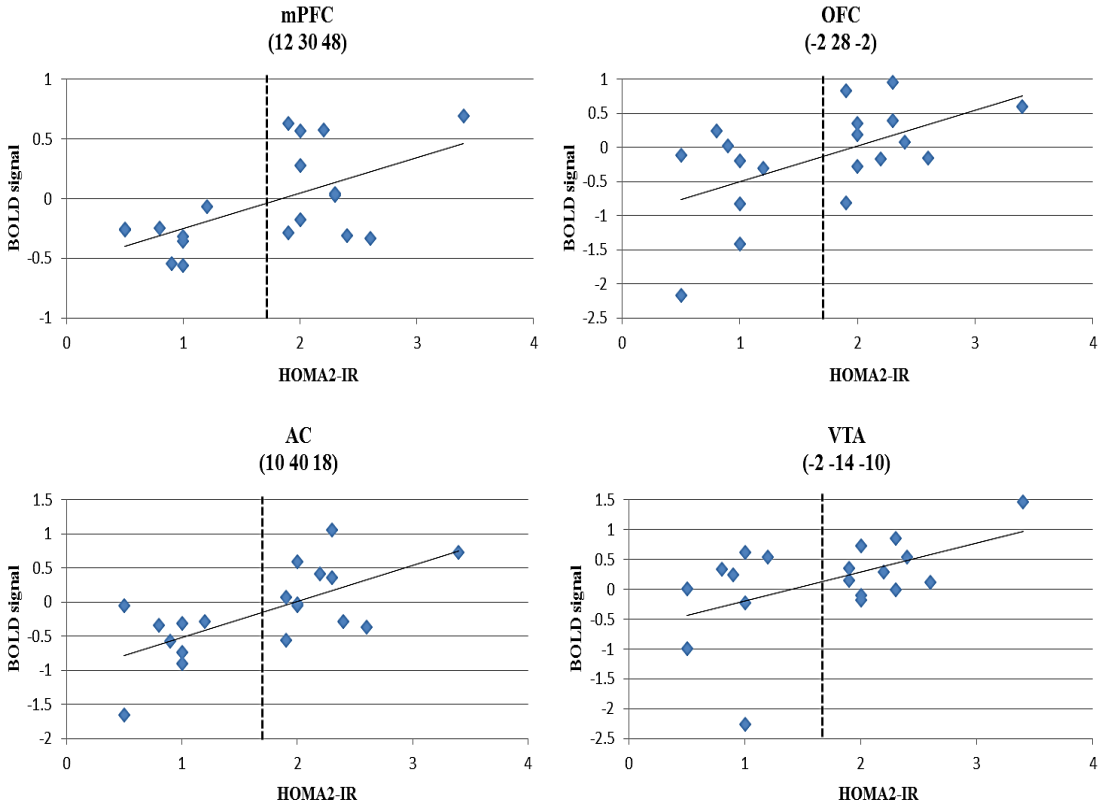

Figure 8: Correlation between insulin resistance and BOLD response in the mPFC, OFC, AC and VTA during a glucose challenge

Parameter estimates for a 5mm radius sphere centered on the peak voxel within some ROIs were extracted for each subject (n= 19) and plotted against HOMA2-IR to examine the relationship between insulin resistance and brain responses to food pictures during a glucose challenge. The dashed line indicates the insulin resistance cutoff as defined by HOMA2-IR. Abbreviations: medial prefrontal cortex (mPFC) orbitofrontal cortex (OFC) anterior cingulate (AC) and ventral tegmental area (VTA).

Table 13 Correlation between insulin resistance and BOLD response to food pictures during glucose vs. water condition

				Glucose>water				
		Without BMI				**With BMI**		
				Positive correlation				
Region	**Hem**	**Cluster (K)**	**t stat**	**MNI coordinates (x y z)**	**Hem**	**Cluster (K)**	**t stat**	**MNI coordinates (x y z)**
HC-C								
DLPFC	L	5	3.98	(-26 28 38)	**L**	**21**	**5.09**	**(-30 14 42)**
					R	**49**	**6.23**	**(24 10 64)**
mPFC					R	13	4.44	(12 32 48)
Midbrain	R	5	4.38	(0 -30 -12)				
Insula	L	8	4.27	(-34 10 16)				
Fusiform	R	36	4.66	(26 -40 -16)				
LC-C								
Midbrain					**R**	**11**	**5.4**	**(12 -26 -16)**
HC-LC								
DLPFC	R	8	4.4	(32 48 10)	L	26	4.39	(-34 52 20)
					R	52	5.3	(32 48 10)
OFC	L	22	4.69	(-34 30 -16)				
Midbrain	R	12	4.45	(0 -28 -12)	R	6	4.71	(4 -34 -4)
Hippocampus					L	8	3.92	(-28 -6 -20)
					R	5	4.39	(16 -36 6)
Amygdala					**L**	**34**	**6.06**	**(-28 -2 -18)**
					R	**17**	**4.63**	**(28 0 -20)**
Fusiform	R	12	3.94	(28 -30 -24)	L	10	5.18	(-30 -64 -18)
					R	29	5.1	(30 -56 -12)

Regions with significant activation by high-calorie (HC) or low-calorie food pictures (LC) vs. control pictures (C), or by HC vs. LC, at a threshold of $p < 0.001$ (uncorrected) with a minimum cluster size of 5 voxels. The regions satisfying the family-wise error (FWE) threshold of $p < 0.05$ (corrected) are highlighted in bold. Contrasts lacking significant effects are not shown. Abbreviations: left (L), right (R), hemisphere (hem), number of voxels in a cluster (k), Montreal Neurological Institute (MNI), body mass index (BMI), and dorsolateral prefrontal cortex (DLPFC), medial prefrontal cortex (mPFC), and orbitofrontal cortex (OFC).

Chapter 4

Discussion

4.1 Key findings in the current study

4.1.1 fMRI results

To our knowledge, this is the first neuroimaging study to investigate the impact of insulin sensitivity on appetitive brain responses to visual food cues following a glucose challenge. The insulin-sensitive and insulin-resistant groups responded differently to food pictures in corticolimbic brain regions associated with cognition, reward, emotion, and control of appetite and ingestive behavior. After water consumption, food pictures elicited limited ROI activation in the insulin-sensitive group, but broad regions of activation in the insulin-resistant group (Table 5). Following the glucose challenge, reactivity to food pictures was significantly inhibited in the insulin-sensitive group, but not in the insulin-resistant group (Table 6), resulting in greater activation in the insulin-resistant group compared to the insulin-sensitive group (Table 9). Lastly, the BOLD response to food pictures in several corticolimbic regions following the glucose challenge correlated with insulin resistance (Table 12).

4.2 Contrasting the current study with previous neuroimaging studies

4.2.1 Brain reactivity to food cues following a glucose challenge

Our observation of an inhibitory effect of a glucose challenge on brain reactivity to food pictures in the insulin-sensitive group (Table 6) is consistent with a recent report that found reduced brain responses to pictures of palatable food following a glucose challenge in normal weight subjects (Kroemer *et al.*, 2012). In their study, BOLD signal was reduced in the basal ganglia and paralimbic regions such as the middle temporal gyrus, anterior

cingulate, and medial frontal gyrus. Also, they reported a negative correlation between insulin concentrations following a glucose challenge and the BOLD response to food pictures in a large bilateral network and the right hemisphere of the limbic system, suggesting that insulin inhibits brain reactivity to food pictures following a glucose challenge. In our study, insulin-sensitive subjects exhibited inhibition of the BOLD signal in the bilateral DLPFC and insula, and in two regions inhibited in Kroemer *et al.*'s study (mPFC and anterior cingulate) in response to food pictures following the glucose challenge, and with the exception of the anterior cingulate, in response to HC (Table 6). A differential response (water>glucose) was found in the OFC, NAc, hypothalamus and fusiform to HC pictures, in the insula to LC pictures, and in the DLPFC, brainstem, and hippocampus to the HC-LC contrast in insulin-sensitive subjects (Table 7). While these regions did not show decreased reactivity to food pictures, they (except the hypothalamus and brainstem) did correlate negatively with increased insulin levels following a glucose challenge in Kroemer *et al.*'s study, which may reflect reduced activity in these regions following glucose administration.

The fact that we demonstrated a significant positive correlation between the degree of insulin resistance and the BOLD response to food pictures following a glucose challenge (Table 12) supports Kroemer *et al.*'s interpretation that insulin inhibits brain reactivity to food pictures after a glucose challenge. Brain regions exhibiting activity that were positively correlated with the degree of insulin resistance in our study but negatively correlated with the insulin concentrations in Kroemer *et al.*'s study included the DLPFC, amygdala, fusiform, insula, hippocampus, OFC, medial frontal gyrus, anterior cingulate and caudate. These brain areas are associated with decision making, emotion, memory,

learning, and food cue processing. This association is particularly interesting as it suggests that insulin resistance might compromise the normal insulin feedback inhibition on appetitive brain regions following a glucose challenge. Therefore, we postulate that the resistance to insulin's anorexigenic effects may predispose individuals to hyperphagia and contribute to the pathogenesis of obesity.

4.2.2 Neuroimaging studies of insulin resistance

There is a limited number of fMRI and other neuroimaging studies that have examined the effect of insulin sensitivity on brain responses to experimental manipulation of insulin and glucose. An fMRI study demonstrated that a glucose challenge inhibited hypothalamic activity in healthy men but not in age-matched men diagnosed with type 2 diabetes (Vidarsdottir *et al.*, 2007). Since the hypothalamus is involved in the regulation of appetite and energy metabolism, the maladaptive hypothalamic response to a glucose challenge may compromise postprandial satiety in individuals with type 2 diabetes—a form of insulin resistance. The insulin-sensitive group in our study showed an inhibition in the hypothalamus in response to HC pictures during the glucose challenge as compared to the water control. On the other hand, inhibition of the hypothalamus was not detected in the insulin-resistant group (Table 7).

A PET study has shown that insulin-induced glucose metabolism in the ventral striatum, PFC and insula was reduced in insulin-resistant compared to insulin-sensitive men (Anthony *et al.*, 2006). Another study found that cortical activity, as measured using magnetoencephalography (MEG) over the course of a hyperinsulinemic-euglycemic clamp study, was negatively correlated with BMI and positively correlated with the degree of insulin sensitivity (Tschritter *et al.*, 2006). He also demonstrated that insulin did not

activate the cortex of subjects with the Gly972Arg polymorphism of the insulin receptor substrate, a genetic condition that predisposes individuals to develop type 2 diabetes. Thus, they proposed that obesity and insulin resistance might be associated with reduced cortical insulin sensitivity through different mechanisms. Currently, it is unclear whether cortical insulin resistance precedes or follows obesity.

The results of the aforementioned studies differ from the current study because the protocols did not include food cues. As well, other methodological, demographic and image analysis differences exist. However, these studies, in addition to ours, indicate that insulin resistance is associated with altered responses in appetite- and reward-related brain regions, suggesting that brain insulin resistance exists concurrent with peripheral insulin resistance.

4.2.3 Is it glucose or insulin that affects brain activity?

The hyperglycemia and hyperinsulinemia that occur concurrently during the first 30 minutes of a glucose challenge constitute two important satiety signals that are also present during the postprandial period (Woods *et al.*, 1990; Baskin *et al.*, 1999; Korner & Leibel, 2003; Woods *et al.*, 2006). Therefore, corticolimbic BOLD responses during a glucose challenge may be related to a change in insulin, glucose, or their combination. Previous studies have measured brain reactivity to food cues while manipulating glucose or insulin concentrations independently. A study by (Page *et al.*, 2011) compared BOLD responses to food pictures during a hyperinsulinemic clamp in lean and obese subjects while euglycemic or hypoglycaemic. Euglycemia was associated with increased reactivity to food pictures in the PFC and anterior cingulate (regions involved in control and motivation) in lean but not obese subjects. In contrast, hypoglycemia was associated with increased

reactivity to HC pictures in limbic-striatal brain regions, including substantia nigra, VTA, striatum, hypothalamus, and thalamus in obese relative to lean subjects. Because insulin levels were maintained at the same level in the two groups, the authors suggested that glucose rather than insulin modulates food cue reactivity of the appetitive network implicated in processing the desire and craving for food (Page *et al.*, 2011).

Conversely, a recent fMRI study used intranasal insulin administration to examine the direct effect of insulin on the brain response to food pictures in lean subjects. This route of administration increased central insulin concentrations in the absence of any changes in peripheral insulin or glucose concentrations (Guthoff *et al.*, 2010). The authors found that, compared to placebo, intranasal insulin administration reduced the BOLD response to food pictures in the bilateral fusiform gyrus, the right hippocampus, the right temporal superior, and frontal middle cortex. Some of these regions overlapped with the regions inhibited by the glucose challenge in the insulin-sensitive group in our study (e.g., bilateral DLPFC and mPFC, right fusiform, and right hippocampus). Since glucose levels were unaffected by intranasal insulin, Guthoff *et al.* suggested that insulin primarily affects responses to food cues. Interestingly, we found that the DLPFC, mPFC, hippocampus and fusiform (among many other regions) were bilaterally activated by food pictures in the insulin-resistant group following the glucose challenge. Moreover, the activity in these regions was positively correlated with the degree of insulin resistance. This suggests that insulin signaling in regions that are implicated in appetite regulation, decision making, food craving, and object recognition was compromised by insulin resistance. It is conceivable that this pattern of central insulin resistance may lead to increased appetite and overconsumption of food.

Another study by the same group, using MEG, examined the brain response to food pictures in lean and obese subjects following intranasal insulin administration (Guthoff *et al.*, 2011). The researchers found that intranasal insulin administration modulated the cerebral response in higher visual areas, especially the fusiform gyrus, to food pictures in lean but not obese subjects. They proposed that obese subjects display a pattern of cerebral insulin resistance, which may contribute to overconsumption of food and the pathogenesis of obesity. Importantly, there was an overlap in brain response regions identified in obese subjects in Guthoff *et al.*'s study and the insulin-resistant subjects, the majority of whom were obese, in our study. In particular, we found a large bilateral BOLD response to food pictures in the fusiform in insulin-resistant subjects following a glucose challenge. Moreover, the BOLD response to HC pictures was greater in the fusiform of insulin-resistant compared to insulin-sensitive subjects following a glucose challenge. Our findings expand on Guttoff *et al.*'s (2011) results by showing that the activity in fusiform (bilaterally) exhibited a positive interaction between study condition and insulin sensitivity, as well as a positive correlation between the degree of insulin resistance and the BOLD response to HC pictures following a glucose challenge. Based on these findings, we suggest that greater activation of the fusiform in response to the HC pictures may reflect increased recognition of appetizing HC pictures in insulin-resistant subjects following a glucose challenge. This may ultimately lead to increased motivational salience and overconsumption of HC food.

Lastly, a recent study examined brain responses to food pictures in patients with type 1 diabetes taking two different forms of insulin: Insulin Detemir (ID), which is more lipophilic and is thus able to cross the BBB more readily than standard insulin forms, and

the Neutral Protamine Hagedorn (NPH) insulin, which is a standard form of insulin. Patients underwent an fMRI scan at the end of a 12-week treatment regimen with either ID or NPH insulin. The BOLD response to food pictures was reduced in the insula following ID as compared to NPH treatment. In addition, treatment with ID, but not NPH, led to a modest reduction in body weight. The authors suggested that the reduction in the BOLD signal in the insula, a region involved in processing food stimuli and food craving, may partly explain the weight reducing effect of ID (Van Golen *et al.*, 2014). These findings are consistent with our results where the reactivity of the insula to food pictures was suppressed by a glucose challenge in the insulin-sensitive group. On the other hand, we found that the insula was significantly activated in response to food pictures in the insulin-resistant group following a glucose challenge and that activation was positively correlated with the degree of insulin resistance. Impaired insulin signaling in the insula may increase the reward value of food in insulin-resistant subjects, which may predispose them to overeating and obesity.

Although it is difficult to integrate the outcomes of previous studies with the current study because of the variations in imaging techniques, protocols and analysis, collectively, these studies suggest that brain responses are influenced by insulin as opposed to (or in addition to) glucose, thereby highlighting the importance of central insulin signaling in appetite regulation. In addition, based on previous studies and our current study, we postulate that despite the exaggerated insulin secretory response in insulin-resistant subjects following a glucose challenge, the brain is less responsive to the inhibitory effect of insulin, resulting in increased responsiveness of the corticolimbic brain to food cues.

4.3 The effect of metabolic condition and adiposity

4.3.1 Neuroimaging studies in fasted vs. fed in normal weight subjects

In the fed state, a rapid physiological change in the concentration of several hormones occurs to induce satiety and terminate food intake (Gibson *et al.*, 2010). Insulin is one of the primary satiety signals in the body. Previous neuroimaging studies have consistently shown that the appetitive network's reactivity to food pictures in normal weight subjects is reduced in the fed compared to fasted state (LaBar *et al.*, 2001; Killgore *et al.*, 2003; Hinton *et al.*, 2004; Holsen *et al.*, 2005; St-Onge *et al.*, 2005; Porubska *et al.*, 2006; Van der Laan *et al.*, 2011). In agreement with those studies, we observed reduced corticolimbic reactivity to food pictures during a glucose challenge condition when compared to the fasted water condition, and this effect was more pronounced in insulin-sensitive subjects. Interestingly, following the glucose challenge, the insulin-resistant group responded more robustly to food pictures than the insulin-sensitive group in several brain regions that exhibit more activation in the fasted compared to fed state in previous studies. Specifically, higher reactivity to food pictures was observed in the DLPFC, mPFC, brainstem, anterior cingulate, insula, caudate, pallidum, and fusiform in the insulin-resistant compared to the insulin-sensitive group (Table 9). Increased activity in corticolimbic regions, which are important for executive control and salience processing, may result from increased attention to food pictures, leading to overconsumption of food or a delay in the termination of food intake in insulin-resistant subjects.

4.3.2 Neuroimaging studies in fasted vs. fed in normal weight vs. obese

Obesity is characterized by increased fasting and postprandial insulin concentrations (Bagdade *et al.*, 1967). Our results complement previous neuroimaging studies, which have

identified differences in the brain response to visual food cues in normal weight compared to obese subjects in fasted vs. fed states (DelParigi A. *et al.*, 2002; Martin *et al.*, 2009; Dimitropoulos *et al.*, 2012). Previous studies have shown that overweight and obese individuals exhibit increased brain responsiveness to food cues compared to normal weight individuals in the mPFC, temporal, and corticolimbic regions (lateral OFC, caudate, anterior cingulate) in the fed state. Furthermore, some studies have shown that, compared to normal weight subjects and baseline conditions, obese subjects, especially those with the extreme obesity phenotype such as seen in PWS, exhibit an increase in corticolimbic brain reactivity, particularly in the amygdala, OFC, mPFC, insula, hippocampus, parahippocampal gyrus, and fusiform when viewing food pictures after eating (Holsen *et al.*, 2006), and in the mPFC following a glucose challenge (Miller *et al.*, 2007). These studies suggest that the postprandial hyper reactivity to food pictures seen in subjects with varying degrees of obesity may result from impaired neural mechanisms regulating satiety and may underlie hyperphagia. Interestingly, there is an overlap between brain regions that were activated in response to food pictures in obese subjects in the fed state and brain regions that were activated in insulin-resistant subjects following a glucose challenge in our study. However, these aforementioned studies focused on the effect of adiposity and did not address the possibility that the differential brain response between obese and lean individuals could be due to different insulin sensitivities.

Recently, an fMRI study by Heni *et al*. compared brain responses to food pictures before, 30 minutes, and 120 minutes following a glucose challenge (vs. a water control) in lean, insulin-sensitive and overweight, insulin-resistant subjects. They found that 120 minutes after glucose ingestion (insulin levels are significantly elevated 120 minute while

glucose levels peak around 30 minutes after ingestion), the reactivity to HC pictures in brain regions in the PFC (DLPFC, OFC, anterior cingulate and parietal cortex) negatively correlated with insulin sensitivity, independent of BMI. That is, while lean, insulin-sensitive subjects had a reduced PFC response to HC pictures, overweight, insulin-resistant subjects had an increased PFC response. These results suggest that insulin resistance in the PFC may be associated with a reduced inhibitory control to HC food cues after caloric intake, which may promote overeating behavior (Heni *et al.*, 2014). Likewise, we observed that reactivity to HC pictures correlated positively with insulin resistance following a glucose challenge in mPFC, OFC, anterior cingulate and VTA. Our results may reflect impaired brain reactivity to HC pictures as a function of insulin resistance in regions thought to regulate inhibitory control, attention, motivation, and emotional processing, which may enhance subjective craving when confronted with rewarding, energy-dense food. This may lead to increased meal frequency and/or delayed meal termination, which may lead to excess energy intake and weight gain.

4.3.3 Is the brain response due to adiposity or insulin sensitivity?

Adiposity was a potential confounder since the insulin-resistant group had a significantly higher average BMI than the insulin-sensitive group (Table 1). Moreover, previous neuroimaging studies have shown that BMI positively correlates with the brain response to food cues (Killgore & Yurgelun-Todd, 2005; Rothemund *et al.*, 2007; Stoeckel *et al.*, 2008; Martin *et al.*, 2009). Therefore, it was important to determine the extent to which our imaging results were influenced by adiposity. This was accomplished by analyzing data after modeling BMI as a nuisance covariate. We found that BMI had a

minimal effect on the results, which suggests that the brain responses seen in our findings are primarily due to insulin sensitivity and not to BMI.

4.4 Study strengths, limitations and future directions

4.4.1 Study strengths

To our knowledge, this is the first study that has investigated how insulin sensitivity affects brain responsiveness to visual food cues during a glucose challenge. This study has several strengths. Firstly, scanning sessions were counterbalanced across subjects to control for potential order effects and were conducted during the afternoon to ensure that a wide variety of a lunch-appropriate food pictures could be presented. Secondly, instead of a baseline scan, we conducted a well-matched water control fMRI scan session to control for feedback effects related to stomach expansion and/or altered esophageal/gastric motility. This control session was done on a separate day to control for habituation to food cues. Finally, we controlled for menstrual cycle phase and adiposity. We identified statistically significant differences with robust effect sizes in the corticolimbic reactivity to food pictures between insulin-sensitive and insulin-resistant groups following a glucose challenge.

4.4.2 Limitations

4.4.2.1 Insulin sensitivity measurement

HOMA2-IR is not the "gold standard" for determining peripheral insulin responsiveness. While the hyperinsulinemic-euglycemic clamp technique is the "gold standard" for determining insulin sensitivity, it is costly and labor intensive, which makes it impractical. Therefore, we utilized the HOMA2-IR method, which is widely used in clinical practice and research (Keskin *et al.*, 2005).

4.4.2.2 Glucose challenge

While a glucose challenge does not produce satiety and does not perfectly mimic the hormonal profile that occurs after eating a meal, it is simple, widely used, and met the needs of our study. Following a glucose challenge, rapid physiological changes in glucose, insulin, and other hormone levels occur, which allowed us to examine the effects of insulin sensitivity on brain response to food pictures under physiological conditions (Woods *et al.*, 1990; Baskin *et al.*, 1999; Korner & Leibel, 2003; Woods *et al.*, 2006). On the other hand, intranasal insulin administration may be superior to the hyperinsulinemic-euglycemic clamp technique, meal consumption, and a glucose challenge because it is simple and circumvents the peripheral hypoglycemic effect of insulin and allows for the selective study of central insulin action.

4.4.3 Future directions

The findings presented in this thesis provide a number of promising avenues for further investigations. Our study did not address whether brain responsiveness to food cues influences ingestive behaviour. Thus, future studies should utilize post-scan measures of food intake in addition to hunger levels. In addition, the effect of BMI on brain responses to food cues independent of the effect of insulin sensitivity warrants further investigation. In the future, studies should also examine brain responsiveness to food cues under a glucose challenge in other conditions characterized by insulin resistance, such as type 2 diabetes. Moreover, since insulin resistance can be ameliorated by treatment, future studies should investigate if improving insulin sensitivity normalizes brain reactivity to appetitive stimuli. Finally, research should focus on understanding the possible mechanism(s) underlying the relationship between insulin resistance and abnormal brain responses to visual food cues

following a glucose challenge and identifying the peripheral signals that interact with appetite regulatory pathways. Findings from these studies will shed light on the effect of insulin sensitivity on brain responses to food cues and will be instrumental in exploring potential neuro-gut-hormonal therapies that aim to reduce appetite and treat obesity and insulin resistance using non-invasive techniques.

4.4.4 Final remarks

We investigated the impact of insulin sensitivity on corticolimbic brain activity in response to appetitive and metabolic cues. Overall, our results support the idea that insulin resistance affects appetite regulation and alters corticolimbic responses to appetitive and metabolic cues. Specifically, we showed that insulin sensitivity affected brain reactivity to food pictures following a glucose challenge, with insulin-resistant subjects displaying increased responsiveness to food pictures in corticolimbic brain areas related to emotion, memory and learning, as compared to insulin-sensitive subjects. In addition, we showed a strong positive correlation between the degree of insulin resistance and the BOLD response in several corticolimbic regions during a glucose challenge. The increased responsiveness to food pictures in regions important for visual attention, reward and motivation, executive control, and cognitive processing in insulin-resistant individuals during postprandial hyperinsulinemia suggests that homeostatic feedback might be impaired in the presence of peripheral insulin resistance, which may increase food consumption and contribute to the pathogenesis of obesity. These findings are important for understanding how insulin resistance alters the brain response to metabolic and visual cues, and will be crucial for developing effective prevention and treatment strategies for obesity.

References

Aguirre GK, Zarahn E, & D'Esposito M (1998). The Variability of Human, BOLD Hemodynamic Responses. *NeuroImage* **8**, 360-369.

Amanti-Kandarakis E & Dunaif A (2012). Insulin Resistance and the Polycystic Ovary Syndrome Revisited: An Update on Mechanisms and Implications. *Endocr Rev* **33**, 981-1030.

Anthony K, Reed LJ, Dunn JT, Bingham E, Hopkins D, Marsden PK, & Amiel SA (2006). Attenuation of Insulin-Evoked Responses in Brain Networks Controlling Appetite and Reward in Insulin Resistance: The Cerebral Basis for Impaired Control of Food Intake in Metabolic Syndrome? *Diabetes* **55**, 2986-2992.

Arthurs OJ & Boniface S (2002). How well do we understand the neural origins of the fMRI BOLD signal? *Trends in Neurosciences* **25**, 27-31.

Bagdade JD, Bierman EL, & Porte D, Jr. (1967). The significance of basal insulin levels in the evaluation of the insulin response to glucose in diabetic and nondiabetic subjects. *J Clin Invest* **46**, 1549-1557.

Baicy K, London ED, Monterosso J, Wong ML, Delibasi T, Sharma A, & Licinio J (2007). From the Cover: Leptin replacement alters brain response to food cues in genetically leptin-deficient adults. *PNAS* **104**, 18276-18279.

Baik JH (2013). Dopamine signaling in food addiction: role of dopamine D2 receptors. *BMB Rep* **46**, 519-526.

Barbas H, Zikopoulos B, & Timbie C (2011). Sensory Pathways and Emotional Context for Action in Primate Prefrontal Cortex. *Biological Psychiatry* **69**, 1133-1139.

Baskin DG, Figlewicz Lattemann D, Seeley RJ, Woods SC, Porte D, Jr., & Schwartz MW (1999). Insulin and leptin: dual adiposity signals to the brain for the regulation of food intake and body weight. *Brain Res* **848**, 114-23.

Baskin DG, Hahn TM, & Schwartz MW (1999). Leptin sensitive neurons in the hypothalamus. *Hormone & Metabolic Research* **31**, 345-350.

Baskin DG, Woods SC, West DB, van HM, Posner BI, Dorsa DM, & Porte D, Jr. (1983). Immunocytochemical detection of insulin in rat hypothalamus and its possible uptake from cerebrospinal fluid. *Endocrinology* **113**, 1818-1825.

Bast T & Feldon J (2003). Hippocampal modulation of sensorimotor processes. *Prog Neurobiol* **70**, 319-345.

Batterham RL, ffytche DH, Rosenthal JM, Zelaya FO, Barker GJ, Withers DJ, & Williams SCR (2007). PYY modulation of cortical and hypothalamic brain areas predicts feeding behaviour in humans. *Nature* **450**, 106-109.

Baxter MG & Murray EA (2002). The amygdala and reward. *Nat Rev Neurosci* **3**, 563-573.

Beaver JD, Lawrence AD, van Ditzhuijzen J, Davis MH, Woods A, & Calder AJ (2006). Individual Differences in Reward Drive Predict Neural Responses to Images of Food. *J Neurosci* **26**, 5160-5166.

Benoit SC, Clegg DJ, Seeley RJ, & Woods SC (2004). Insulin and Leptin as Adiposity Signals. *Recent Prog Horm Res* **59**, 267-285.

Berthoud HR, Lenard NR, & Shin AC (2011). Food reward, hyperphagia, and obesity. *American Journal of Physiology-Regulatory, Integrative and Comparative Physiology* **300**, R1266-R1277.

Broadwell RD & Brightman MW (1976). Entry of peroxidase into neurons of the central and peripheral nervous systems from extracerebral and cerebral blood. *J Comp Neurol* **166**, 257-283.

Broberger C, Landry M, Wong H, Walsh JN, & Hokfelt T (1997). Subtypes Y1 and Y2 of the neuropeptide Y receptor are respectively expressed in pro-opiomelanocortin- and neuropeptide-Y-containing neurons of the rat hypothalamic arcuate nucleus. *Neuroendocrinology* **66**, 393-408.

Bruning JC, Gautam D, Burks DJ, Gillette J, Schubert M, Orban PC, Klein R, Krone W, Muller-Wieland D, & Kahn CR (2000). Role of Brain Insulin Receptor in Control of Body Weight and Reproduction. *Science* **289**, 2122-2125.

Cardinal RN, Parkinson JA, Hall J, & Everitt BJ (2002). Emotion and motivation: the role of the amygdala, ventral striatum, and prefrontal cortex. *Neuroscience & Biobehavioral Reviews* **26**, 321-352.

Carnell S, Gibson C, Benson L, Ochner CN, & Geliebter A (2012). Neuroimaging and obesity: current knowledge and future directions. *Obesity Reviews* **13**, 43-56.

Cauda F, D'Agata F, Sacco K, Duca S, Geminiani G, & Vercelli A (2011). Functional connectivity of the insula in the resting brain. *NeuroImage* **55**, 8-23.

Chicurel M (2000). Whatever happened to leptin? *Nature* **404**, 538-540.

Christophe J (1998). Is there appetite after glp-1 and pacap? *Ann N Y Acad Sci* **865**, 323-35.

Cone RD, Cowley MA, Butler AA, Fan W, Marks DL, & Low MJ (2001). The arcuate nucleus as a conduit for diverse signals relevant to energy homeostasis. *Int J Obes Relat Metab Disord* **25 Suppl 5**, S63-S67.

Cornier MA, Von Kaenel SS, Bessesen DH, & Tregellas JR (2007). Effects of overfeeding on the neuronal response to visual food cues. *The American Journal of Clinical Nutrition* **86**, 965-971.

Cowley MA, Smart JL, Rubinstein M, Cerdan MG, Diano S, Horvath TL, Cone RD, & Low MJ (2001). Leptin activates anorexigenic POMC neurons through a neural network in the arcuate nucleus. *Nature* **411**, 480-484.

Cummings DE & Overduin J (2007). Gastrointestinal regulation of food intake. *J Clin Invest* **117**, 13-23.

Del Parigi A, Chen K, Salbe AD, Reiman EM, & Tataranni PA (2003). Are We Addicted to Food? *Obesity Res* **11**, 493-495.

DelParigi A., Chen K, Gautier JF, Salbe AD, Pratley RE, Ravussin E, Reiman EM, & Tataranni PA (2002). Sex differences in the human brain's response to hunger and satiation. *Am J Clin Nutr* **75**, 1017-1022.

Dimitropoulos A, Tkach J, Ho A, & Kennedy J (2012). Greater corticolimbic activation to high-calorie food cues after eating in obese vs. normal-weight adults. *Appetite* **58**, 303-312.

Douketis JD, Paradis G, Keller H, & Martineau C (2005). Canadian guidelines for body weight classification in adults: application in clinical practice to screen for overweight and obesity and to assess disease risk. *CMAJ* **172**, 995-998.

Dunaif A (1997). Insulin resistance and the polycystic ovary syndrome: mechanism and implications for pathogenesis. *Endocr Rev* **18**, 774-800.

Dunaif A, Segal KR, Futterweit W, & Dobrjansky A (1989). Profound peripheral insulin resistance, independent of obesity, in polycystic ovary syndrome. *Diabetes* **38**, 1165-1174.

Elias CF, Aschkenasi C, Lee C, Kelly J, Ahima RS, Bjorbaek C, Flier JS, Saper CB, & Elmquist JK (1999). Leptin differentially regulates NPY and POMC neurons projecting to the lateral hypothalamic area. *Neuron* **23**, 775-786.

Elias CF, Lee C, Kelly J, Aschkenasi C, Ahima RS, Couceyro PR, Kuhar MJ, Saper CB, & Elmquist JK (1998). Leptin Activates Hypothalamic CART Neurons Projecting to the Spinal Cord. *Neuron* **21**, 1375-1385.

Elmquist JK, Bjorbaek C, Ahima RS, Flier JS, & Saper CB (1998). Distributions of leptin receptor mRNA isoforms in the rat brain. *J Comp Neurol* **395**, 535-547.

Esch T & Stefano GB (2004). The neurobiology of pleasure, reward processes, addiction and their health implications. *Neuro Endocrinol Lett* **25**, 235-251.

Farooqi IS, Bullmore E, Keogh J, Gillard J, O'Rahilly S, & Fletcher PC (2007). Leptin Regulates Striatal Regions and Human Eating Behavior. *Science* **317**, 1355.

Figlewicz DP, Sipols AJ, Seeley RJ, Chavez M, Woods SC, & Porte D, Jr. (1995). Intraventricular insulin enhances the meal-suppressive efficacy of intraventricular cholecystokinin octapeptide in the baboon. *Behav Neurosci* **109**, 567-569.

Finkelstein EA, Trogdon JG, Cohen JW, & Dietz W (2009). Annual medical spending attributable to obesity: payer-and service-specific estimates. *Health Aff (Millwood)* **28**, w822-w831.

Finkelstein EA, Khavjou OA, Thompson H, Trogdon JG, Pan L, Sherry B, & Dietz W (2012). Obesity and Severe Obesity Forecasts Through 2030. *American Journal of Preventive Medicine* **42**, 563-570.

Foster LA, Ames NK, & Emery RS (1991). Food intake and serum insulin responses to intraventricular infusions of insulin and IGF-I. *Physiology & Behavior* **50**, 745-749.

Frank S, Kullmann S, & Veit R (2013). Food related processes in the insular cortex. *Frontiers in Human Neuroscience* **7**.

Fry M, Hoyda TD, & Ferguson AV (2007). Making sense of it: roles of the sensory circumventricular organs in feeding and regulation of energy homeostasis. *Experimental Biology and Medicine* **232**, 14-26.

Fuhrer D, Zysset S, & Stumvoll M (2008). Brain Activity in Hunger and Satiety: An Exploratory Visually Stimulated fMRI Study. *Obesity Res* **16**, 945-950.

Fulton S (2010). Appetite and reward. *Frontiers in Neuroendocrinology* **31**, 85-103.

Garner DM & Garfinkel PE (1979). The Eating Attitudes Test: an index of the symptoms of anorexia nervosa. *Psychol Med* **9**, 273-279.

Garner DM, Olmsted MP, Bohr Y, & Garfinkel PE (1982). The Eating Attitudes Test: psychometric features and clinical correlates. *Psychological Medicine* **12**, 871-878.

Geloneze B, Vasques ACJ, Stabe CFC, Pareja JC, Rosado LEFPdL, Queiroz ECd, & Tambascia MA (2009). HOMA1-IR and HOMA2-IR indexes in identifying insulin resistance and metabolic syndrome: Brazilian Metabolic Syndrome Study (BRAMS). *Arquivos Brasileiros de Endocrinologia & Metabologia* **53**, 281-287.

Gibson CD, Carnell S, Ochner CN, & Geliebter A (2010). Neuroimaging, gut peptides and obesity: novel studies of the neurobiology of appetite. *J Neuroendocrinol* **22**, 833-845.

Guthoff M, Stingl KT, Tschritter O, Rogic M, Heni M, Stingl K, Hallschmid M, Haring HU, Fritsche A, Preissl H, & Hennige AM (2011). The insulin-mediated modulation of visually evoked magnetic fields is reduced in obese subjects. *PLoS One* **6**, e19482.

Guthoff M, Grichisch Y, Canova C, Tschritter O, Veit R, Hallschmid M, Haring HU, Preissl H, Hennige AM, & Fritsche A (2010). Insulin Modulates Food-Related Activity in the Central Nervous System. *Journal of Clinical Endocrinology & Metabolism* **95**, 748-755.

Haber SN & Knutson B (2010). The reward circuit: linking primate anatomy and human imaging. *Neuropsychopharmacology* **35**, 4-26.

Halatchev IG, Ellacott KL, Fan W, & Cone RD (2004). Peptide YY3-36 inhibits food intake in mice through a melanocortin-4 receptor-independent mechanism. *Endocrinology* **145**, 2585-2590.

Hallschmid M, Higgs S, Thienel M, Ott V, & Lehnert H (2012). Postprandial Administration of Intranasal Insulin Intensifies Satiety and Reduces Intake of Palatable Snacks in Women. *Diabetes* **61**, 782-789.

Hare TA, Camerer CF, & Rangel A (2009). Self-Control in Decision-Making Involves Modulation of the vmPFC Valuation System. *Science* **324**, 646-648.

Havel PJ (2001). Peripheral Signals Conveying Metabolic Information to the Brain: Short-Term and Long-Term Regulation of Food Intake and Energy Homeostasis. *Experimental Biology and Medicine* **226**, 963-977.

Heni M, Kullmann S, Ketterer C, Guthoff M, Bayer M, Staiger H, Machicao F, Haring HU, Preissl H, Veit R, & Fritsche A (2014). Differential effect of glucose ingestion on the neural processing of food stimuli in lean and overweight adults. *Hum Brain Mapp* **35**, 918-928.

Hinton EC, Parkinson JA, Holland AJ, Arana FS, Roberts C, & Owen AM (2004). Neural contributions to the motivational control of appetite in humans. *European Journal of Neuroscience* **20**, 1411-1418.

Holsen LM, Zarcone JR, Brooks WM, Butler MG, Thompson TI, Ahluwalia JS, Nollen NL, & Savage CR (2006). Neural mechanisms underlying hyperphagia in Prader-Willi Syndrome. *Obesity Res* **14**, 1028-1037.

Holsen LM, Zarcone JR, Thompson TI, Brooks WM, Anderson MF, Ahluwalia JS, Nollen NL, & Savage CR (2005). Neural mechanisms underlying food motivation in children and adolescents. *NeuroImage* **27**, 669-676.

Huerta CI, Sarkar PR, Duong TQ, Laird AR, & Fox PT (2013). Neural bases of food perception: Coordinate-based meta-analyses of neuroimaging studies in multiple modalities. *Obesity Res* n/a.

Huettel SA, Song AW, & McCarthy G (2004). *Functional magnetic resonance imaging*, 1 ed. Sinauer Associates Sunderland.

Kelley AE (2004). Ventral striatal control of appetitive motivation: role in ingestive behavior and reward-related learning. *Neuroscience & Biobehavioral Reviews* **27**, 765-776.

Keskin M, Kurtoglu S, Kendirci M, Atabek ME, & Yazici C (2005). Homeostasis Model Assessment Is More Reliable Than the Fasting Glucose/Insulin Ratio and Quantitative Insulin Sensitivity Check Index for Assessing Insulin Resistance Among Obese Children and Adolescents. *Pediatrics* **115**, e500-e503.

Killgore WD & Yurgelun-Todd DA (2005). Body mass predicts orbitofrontal activity during visual presentations of high-calorie foods. *Neuroreport* **16**, 859-863.

Killgore WD & Yurgelun-Todd DA (2006). Affect modulates appetite-related brain activity to images of food. *Int J Eat Disord* **39**, 357-363.

Killgore WDS, Young AD, Femia LA, Bogorodzki P, Rogowska J, & Yurgelun-Todd DA (2003). Cortical and limbic activation during viewing of high- versus low-calorie foods. *NeuroImage* **19**, 1381-1394.

Kleinridders A, Ferris HA, Cai W, & Kahn CR (2014). Insulin action in brain regulates systemic metabolism and brain function. *Diabetes* **63**, 2232-2243.

Koob GF & Volkow ND (2009). Neurocircuitry of Addiction. *Neuropsychopharmacology* **35**, 217-238.

Korner J & Leibel RL (2003). To eat or not to eat - how the gut talks to the brain. *N Engl J Med* **349**, 926-928.

Kroemer NB, Krebs L, Kobiella A, Grimm O, Vollstadt-Klein S, Wolfensteller U, Kling R, Bidlingmaier M, Zimmermann US, & Smolka MN (2012). (Still) longing for food: Insulin reactivity modulates response to food pictures. *Hum Brain Mapp* n/a.

LaBar KS, Gitelman DR, Parrish TB, Kim YH, Nobre AC, & Mesulam MM (2001). Hunger selectively modulates corticolimbic activation to food stimuli in humans. *Behav Neurosci* **115**, 493-500.

Lindquist MA (2008). The statistical analysis of fMRI data. *Statistical Science* **23**, 439-464.

Liu Y, Gao JH, Liu HL, & Fox PT (2000). The temporal response of the brain after eating revealed by functional MRI. *Nature* **405**, 1058-1062.

Lo JC, Feigenbaum SL, Yang J, Pressman AR, Selby JV, & Go AS (2006). Epidemiology and adverse cardiovascular risk profile of diagnosed polycystic ovary syndrome. *J Clin Endocrinol Metab* **91**, 1357-1363.

Logothetis NK & Wandell BA (2004). Interpreting the BOLD Signal. *Annual Review of Physiology* **66**, 735-769.

Mahankali S, Liu Y, Pu Y, Wang J, Chen CW, Fox PT, & Gao JH (2000). In vivo fMRI demonstration of hypothalamic function following intraperitoneal glucose administration in a rat model. *Magn Reson Med* **43**, 155-159.

Maldjian JA, Laurienti PJ, Kraft RA, & Burdette JH (2003). An automated method for neuroanatomic and cytoarchitectonic atlas-based interrogation of fMRI data sets. *NeuroImage* **19**, 1233-1239.

Malik S, McGlone F, Bedrossian D, & Dagher A (2008). Ghrelin Modulates Brain Activity in Areas that Control Appetitive Behavior. *Cell Metabolism* **7**, 400-409.

Malonek D & Grinvald A (1996). Interactions between electrical activity and cortical microcirculation revealed by imaging spectroscopy: implications for functional brain mapping. *Science* **272**, 551-554.

Marsh C, Berent-Spillson A, Love T, Persad CC, Pop-Busui R, Zubieta JK, & Smith YR (2013). Functional neuroimaging of emotional processing in women with polycystic ovary syndrome: a case-control pilot study. *Fertility and Sterility* **100**, 200-207.

Martin LE, Holsen LM, Chambers RJ, Bruce AS, Brooks WM, Zarcone JR, Butler MG, & Savage CR (2009). Neural Mechanisms Associated With Food Motivation in Obese and Healthy Weight Adults. *Obesity Res* **18**, 254-260.

Matsuda M, Liu Y, Mahankali S, Pu Y, Mahankali A, Wang J, DeFronzo RA, Fox PT, & Gao JH (1999). Altered hypothalamic function in response to glucose ingestion in obese humans. *Diabetes* **48**, 1801-1806.

Mercer JG, Hoggard N, Williams LM, Lawrence CB, Hannah LT, & Trayhurn P (1996). Localization of leptin receptor mRNA and the long form splice variant (Ob-Rb) in mouse hypothalamus and adjacent brain regions by in situ hybridization. *FEBS Letters* **387**, 113-116.

Miller EK (1999). The Prefrontal Cortex: Complex Neural Properties for Complex Behavior. *Neuron* **22**, 15-17.

Miller JL, James GA, Goldstone AP, Couch JA, He G, Driscoll DJ, & Liu Y (2007). Enhanced activation of reward mediating prefrontal regions in response to food stimuli in PraderΓÇôWilli syndrome. *Journal of Neurology, Neurosurgery & Psychiatry* **78**, 615-619.

Mogenson GJ, Jones DL, & Yim CY (1980). From motivation to action: Functional interface between the limbic system and the motor system. *Progress in Neurobiology* **14**, 69-97.

Mokdad AH, Ford ES, Bowman BA, Dietz WH, Vinicor F, Bales VS, & Marks JS (2003). Prevalence of Obesity, Diabetes, and Obesity-Related Health Risk Factors, 2001. *JAMA* **289**, 76-79.

Monti MM (2011). Statistical Analysis of fMRI Time-Series: A Critical Review of the GLM Approach. *Front Hum Neurosci* **5**, 28.

Moran LJ, Misso ML, Wild RA, & Norman RJ (2010). Impaired glucose tolerance, type 2 diabetes and metabolic syndrome in polycystic ovary syndrome: a systematic review and meta-analysis. *Hum Reprod Update* **16**, 347-363.

Morgane PJ, Galler JR, & Mokler DJ (2005). A review of systems and networks of the limbic forebrain/limbic midbrain. *Prog Neurobiol* **75**, 143-160.

Nair DG (2005). About being BOLD. *Brain Research Reviews* **50**, 229-243.

Ogawa S, Lee TM, Nayak AS, & Glynn P (1990). Oxygenation-sensitive contrast in magnetic resonance image of rodent brain at high magnetic fields. *Magn Reson Med* **14**, 68-78.

Page KA, Seo D, Belfort-DeAguiar R, Lacadie C, Dzuira J, Naik S, Amarnath S, Constable RT, Sherwin RS, & Sinha R (2011). Circulating glucose levels modulate neural control of desire for high-calorie foods in humans. *J Clin Invest* **121**, 4161-4169.

PCOS Consensus Workshop Group 2 (2004). Revised 2003 consensus on diagnostic criteria and long-term health risks related to polycystic ovary syndrome (PCOS). *Hum Reprod* **19**, 41-47.

Pelchat ML, Johnson A, Chan R, Valdez J, & Ragland JD (2004). Images of desire: food-craving activation during fMRI. *NeuroImage* **23**, 1486-1493.

Porubska K, Veit R, Preissl H, Fritsche A, & Birbaumer N (2006). Subjective feeling of appetite modulates brain activity: An fMRI study. *NeuroImage* **32**, 1273-1280.

Powley TL & Phillips RJ (2004). Gastric satiation is volumetric, intestinal satiation is nutritive. *Physiology & Behavior* **82**, 69-74.

Risinger RC, Salmeron BJ, Ross TJ, Amen SL, Sanfilipo M, Hoffmann RG, Bloom AS, Garavan H, & Stein EA (2005). Neural correlates of high and craving during cocaine self-administration using BOLD fMRI. *NeuroImage* **26**, 1097-1108.

Rolls ET (2011). Taste, olfactory and food texture reward processing in the brain and obesity. *Int J Obes* **35**, 550-561.

Rolls ET, Burton MJ, & Mora F (1980). Neurophysiological analysis of brain-stimulation reward in the monkey. *Brain Research* **194**, 339-357.

Rolls ET & McCabe C (2007). Enhanced affective brain representations of chocolate in cravers vs. non-cravers. *Eur J Neurosci* **26**, 1067-1076.

Rosenbaum M, Sy M, Pavlovich K, Leibel RL, & Hirsch J (2008). Leptin reverses weight loss-induced changes in regional neural activity responses to visual food stimuli. *J Clin Invest* **118**, 2583-2591.

Rothemund Y, Preuschhof C, Bohner G, Bauknecht HC, Klingebiel R, Flor H, & Klapp BF (2007). Differential activation of the dorsal striatum by high-calorie visual food stimuli in obese individuals. *NeuroImage* **37**, 410-421.

Safar FH, Mojiminiyi OA, Al-Rumaih HM, & Diejomaoh MF (2011). Computational Methods Are Significant Determinants of the Associations and Definitions of Insulin Resistance Using the Homeostasis Model Assessment in Women of Reproductive Age. *Clinical Chemistry* **57**, 279-285.

Sah P, Faber ES, Lopez De AM, & Power J (2003). The amygdaloid complex: anatomy and physiology. *Physiol Rev* **83**, 803-834.

Sam AH, Troke RC, Tan TM, & Bewick GA (2012). The role of the gut/brain axis in modulating food intake. *Neuropharmacology* **63**, 46-56.

Schoenbaum G, Chiba AA, & Gallagher M (1998). Orbitofrontal cortex and basolateral amygdala encode expected outcome during learning. *Nature Neurosci* **1**, 155-159.

Schöfl C, Horn Rê, Schill T, Schlösser HW, Müller MJ, & Brabant G (2002). Circulating ghrelin levels in patients with polycystic ovary syndrome. *The Journal of Clinical Endocrinology & Metabolism* **87**, 4607-4610.

Schulingkamp RJ, Pagano TC, Hung D, & Raffa RB (2000). Insulin receptors and insulin action in the brain: review and clinical implications. *Neuroscience & Biobehavioral Reviews* **24**, 855-872.

Schwartz MW, Seeley RJ, Campfield LA, Burn P, & Baskin DG (1996). Identification of targets of leptin action in rat hypothalamus. *J Clin Invest* **98**, 1101-1106.

Schwartz MW, Seeley RJ, Woods SC, Weigle DS, Campfield LA, Burn P, & Baskin DG (1997). Leptin increases hypothalamic pro-opiomelanocortin mrna expression in the rostral arcuate nucleus. *Diabetes* **46**, 2119-2123.

Schwartz MW, Sipols AJ, Marks JL, Sanacora G, White JD, Scheurink A, Kahn SE, Baskin DG, Woods SC, & Figlewicz DP (1992). Inhibition of hypothalamic neuropeptide Y gene expression by insulin. *Endocrinology* **130**, 3608-3616.

Sescousse G, Redout J, & Dreher JC (2010). The Architecture of Reward Value Coding in the Human Orbitofrontal Cortex. *The Journal of Neuroscience* **30**, 13095-13104.

Siep N, Roefs A, Roebroeck A, Havermans R, Bonte ML, & Jansen A (2009). Hunger is the best spice: an fMRI study of the effects of attention, hunger and calorie content on food reward processing in the amygdala and orbitofrontal cortex. *Behav Brain Res* **198**, 149-158.

Simansky KJ (2005). NIH symposium series: Ingestive mechanisms in obesity, substance abuse and mental disorders. *Physiology & Behavior* **86**, 1-4.

Small DM (2006). Central gustatory processing in humans. *Adv Otorhinolaryngol* **63**, 191-220.

Smeets PAM, de Graaf C, Stafleu A, van Osch MJP, & van der Grond J (2005). Functional MRI of human hypothalamic responses following glucose ingestion. *NeuroImage* **24**, 363-368.

Spiegelman BM & Flier JS (2001). Obesity and the Regulation of Energy Balance. *Cell* **104**, 531-543.

Statistics Canada (2010). Fitness of Canadian adults: Results from the 2007-2009 Canadian Health Measures Survey. Available at: http://www.statcan.gc.ca/pub/82-003-x/2010001/article/11064/key-cle-eng.htm [Accessed April 22, 2015]

Statistics Canada (2012). Overweight and obesity in children and adolescents: Results from the 2009 to 2011 Canadian Health Measures Survey. Available at: http://www.statcan.gc.ca/pub/82-003-x/2012003/article/11706/abstract-resultat-eng.htm [Accessed April 22, 2015]

St-Onge MP, Sy M, Heymsfield SB, & Hirsch J (2005). Human Cortical Specialization for Food: a Functional Magnetic Resonance Imaging Investigation. *J Nutr* **135**, 1014-1018.

Stice E, Yokum S, Zald D, & Dagher A (2011). Dopamine-Based Reward Circuitry Responsivity, Genetics, and Overeating. In *Behavioral Neurobiology of Eating Disorders*, eds. Adan RAH & Kaye WH, pp. 81-93. Springer Berlin Heidelberg.

Stoeckel LE, Weller RE, Cook EW, III, Twieg DB, Knowlton RC, & Cox JE (2008). Widespread reward-system activation in obese women in response to pictures of high-calorie foods. *NeuroImage* **41**, 636-647.

Strubbe JH, Porte D, & Woods SC (1988). Insulin responses and glucose levels in plasma and cerebrospinal fluid during fasting and refeeding in the rat. *Physiology & Behavior* **44**, 205-208.

Suzuki K, Jayasena CN, & Bloom SR (2011). The Gut Hormones in Appetite Regulation. *J Obes* **2011**, 528401.

Tang DW, Fellows LK, Small DM, & Dagher A (2012). Food and drug cues activate similar brain regions: A meta-analysis of functional MRI studies. *Physiology & Behavior* **106**, 317-324.

Tomasi D, Wang GJ, Wang R, Backus W, Geliebter A, Telang F, Jayne MC, Wong C, Fowler JS, & Volkow ND (2009). Association of body mass and brain activation during gastric distention: implications for obesity. *PLoS One* **4**, e6847.

Tschritter O, Preissl H, Hennige AM, Stumvoll M, Porubska K, Frost R, Marx H, Klosel B, Lutzenberger W, Birbaumer N, Haring HU, & Fritsche A (2006). The cerebrocortical response to hyperinsulinemia is reduced in overweight humans: A magnetoencephalographic study. *PNAS* **103**, 12103-12108.

Van der Laan LN, de Ridder DTD, Viergever MA, & Smeets PAM (2011). The first taste is always with the eyes: A meta-analysis on the neural correlates of processing visual food cues. *NeuroImage* **55**, 296-303.

Van Golen LW, Veltman DJ, IJzerman RG, Deijen JB, Heijboer AC, Barkhof F, Drent ML, & Diamant M (2014). Effects of insulin detemir and NPH insulin on body weight and appetite-regulating brain regions in human type 1 diabetes: a randomized controlled trial. *PLoS One* **9**, e94483.

Van Vugt DA, Krzemien A, Alsaadi H, Frank TC, & Reid RL (2014). Glucose-induced inhibition of the appetitive brain response to visual food cues in polycystic ovary syndrome patients. *Brain Res* **1558**, 44-56.

Van Vugt DA, Krzemien AA, Alsaadi H, Palerme S, & Reid RL (2012). Effect of insulin sensitivity on corticolimbic responses to food picture in women with polycystic ovary syndrome. *Obesity Res* **in press**.

Van Vugt DA (2010). Brain imaging studies of appetite in the context of obesity and the menstrual cycle. *Hum Reprod Update* **16**, 276-292.

Vidarsdottir S, Smeets PAM, Eichelsheim DL, van Osch MJP, Viergever MA, Romijn JA, van der Grond J, & Pijl H (2007). Glucose Ingestion Fails to Inhibit Hypothalamic Neuronal Activity in Patients With Type 2 Diabetes. *Diabetes* **56**, 2547-2550.

Volkow ND & Wise RA (2005). How can drug addiction help us understand obesity? *Nat Neurosci* **8**, 555-560.

Wallner-Liebmann S, Koschutnig K, Reishofer G, Sorantin E, Blaschitz B, Kruschitz R, Unterrainer HF, Gasser R, Freytag F, Bauer-Denk C, & Mangge H (2010). Insulin and Hippocampus Activation in Response to Images of High-Calorie Food in Normal Weight and Obese Adolescents. *Obesity Res* **18**, 1552-1557.

Wang GJ, Volkow ND, Logan J, Pappas NR, Wong CT, Zhu W, Netusll N, & Fowler JS (2001). Brain dopamine and obesity. *The Lancet* **357**, 354-357.

Watanabe M (1996). Reward expectancy in primate prefrontal neurons. *Nature* **382**, 629-632.

Whitaker RC, Wright JA, Pepe MS, Seidel KD, & Dietz WH (1997). Predicting Obesity in Young Adulthood from Childhood and Parental Obesity. *New England Journal of Medicine* **337**, 869-873.

Wittmann BC, Schott BrH, Guderian S, Frey JU, Heinze HJ, & Duzel E (2005). Reward-Related fMRI Activation of Dopaminergic Midbrain Is Associated with Enhanced Hippocampus- Dependent Long-Term Memory Formation. *Neuron* **45**, 459-467.

Woods SC, Figlewicz Lattemann DP, Schwartz MW, & Porte D, Jr. (1990). A re-assessment of the regulation of adiposity and appetite by the brain insulin system. *Int J Obes* **14 Suppl 3:69-73; discussion 74-6.**, 69-73.

Woods SC, Lotter EC, McKay LD, & Porte D, Jr. (1979). Chronic intracerebroventricular infusion of insulin reduces food intake and body weight of baboons. *Nature* **282**, 503-505.

Woods SC, Benoit SC, & Clegg DJ (2006a). The Brain-Gut-Islet Connection. *Diabetes* **55**, S114-S121.

World Health Organization (2015). Obesity and overweight. Media Centre Fact Sheet N°311. Available at: http://www.who.int/mediacentre/factsheets/fs311/en/ [Accessed April 22, 2015]

Wren AM & Bloom SR (2007). Gut Hormones and Appetite Control. *Gastroenterology* **132**, 2116-2130.

Zahm DS (2000). An integrative neuroanatomical perspective on some subcortical substrates of adaptive responding with emphasis on the nucleus accumbens. *Neurosci Biobehav Rev* **24**, 85-105.

Zhang Y, Proenca R, Maffei M, Barone M, Leopold L, & Friedman JM (1994). Positional cloning of the mouse obese gene and its human homologue. *Nature* **372**, 425-32.

Zigman JM, Jones JE, Lee CE, Saper CB, & Elmquist JK (2006). Expression of ghrelin receptor mRNA in the rat and the mouse brain. *J Comp Neurol* **494**, 528-548.

Appendix A

Eating Attitudes Test (EAT-26)

Age: **Current Weight:** **Height:**

Highest Adult Weight: **Lowest Adult Weight:**

Please choose one response by marking the checkbox to the right for each of the following statements	**Always**	**Usually**	**Often**	**Some times**	**Rarely**	**Never**	Score
1. Am terrified about being overweight.	☐	☐	☐	☐	☐	☐	
2. Avoid eating when I am hungry.	☐	☐	☐	☐	☐	☐	
3. Find myself preoccupied with food.	☐	☐	☐	☐	☐	☐	
4. Have gone on eating binges where I feel that I may not be able to stop.	☐	☐	☐	☐	☐	☐	
5. Cut my food into small pieces.	☐	☐	☐	☐	☐	☐	
6. Aware of the calorie content of foods that I eat.	☐	☐	☐	☐	☐	☐	
7. Particularly avoid food with a high carbohydrate content (i.e. bread, potatoes, etc).	☐	☐	☐	☐	☐	☐	
8. Feel that others would prefer if I ate more.	☐	☐	☐	☐	☐	☐	
9. Vomit after I have eaten.	☐	☐	☐	☐	☐	☐	
10. Feel extremely guilty after eating.	☐	☐	☐	☐	☐	☐	
11. Am preoccupied with a desire to be thinner.	☐	☐	☐	☐	☐	☐	
12. Think about burning up calories when I exercise.	☐	☐	☐	☐	☐	☐	
13. Other people think that I am too thin.	☐	☐	☐	☐	☐	☐	
14. Am preoccupied with the thought of having fat on my body.	☐	☐	☐	☐	☐	☐	
15. Take longer then others to eat my meals.	☐	☐	☐	☐	☐	☐	
16. Avoid food with sugar in them.	☐	☐	☐	☐	☐	☐	
17. Eat diet foods.	☐	☐	☐	☐	☐	☐	
18. Feel that food controls my life.	☐	☐	☐	☐	☐	☐	
19. Display self-control around food.	☐	☐	☐	☐	☐	☐	
20. Feel that others pressure me to eat.	☐	☐	☐	☐	☐	☐	
21. Give too much time and thought to food.	☐	☐	☐	☐	☐	☐	

22. Feel uncomfortable after eating sweets.	☐☐☐☐☐☐	
23. Engage in dieting behavior.	☐☐☐☐☐☐	
24. Like my stomach to be empty.	☐☐☐☐☐☐	
25. Have the impulse to vomit after meals.	☐☐☐☐☐☐	
26. Enjoy trying new rich foods.	☐☐☐☐☐☐	

1) Have you gone on eating binges where you feel that you may not be able to stop? (Eating much more than most people would eat under the same circumstances).
   ☐ No ☐ Yes How many times in the last 6 months?

2) Have you ever made yourself sick (vomited) to control your weight or shape?
   ☐ No ☐ Yes How many times in the last 6 months?

3) Have you ever used laxatives, diet pills or diuretics (water pills) to control your weight or shape?
   ☐ No ☐ Yes How many times in the last 6 months?

4) Have you ever been treated for an eating disorder?
   ☐ No ☐ Yes When?

Appendix B

Queen's MRI Checklist

Centre for Neuroscience Studies

fMRI Facility

MAGNETIC RESONANCE (MR)ENVIRONMENT SAFETY CHECKLIST FOR INDIVIDUALS

This MR system has a very strong magnetic field (3 Tesla) that may be hazardous to individuals entering the magnet room if they have certain metallic, electronic, magnetic, or mechanical implants, devices or objects. Therefore, all individuals are required to fill out this form BEFORE entering the magnet room. Be advised, the magnet is ALWAYS ON. This questionnaire must be completed accurately to ensure safety. An answer of "Yes" in a category may not necessarily exclude you from entry into the MRI or its vicinity.

Please Circle

Have you had prior surgery or an operation (e.g. athroscopy, endoscopy, etc) of any kind? Yes No
Have you had an injury to the eye involving a metallic object (e.g. metallic slivers, foreign body)? Yes No
Have you ever been injured by a metallic object or foreign body (e.g. BB, bullet, shrapnel, etc.)? Yes No
Are you pregnant or suspect that you are pregnant? Yes No

WARNING: Certain implants, devices or objects may be hazardous to you in the MR environment or the magnet room. DO NOT ENTER the MR environment or the magnet room if you have any questions or concern regarding an implant, device object.

Please indicate if you have any of the following:

Yes No Aneurysm clip(s)
Yes No Cardiac pacemaker
Yes No Implanted cardioverter defibrillator (ICD)
Yes No Electronic implant or device
Yes No Magnetically-activated implant or device
Yes No Neurostimulation system
Yes No Spinal cord stimulator
Yes No Cochlear implant or implanted hearing aid
Yes No Insulin or infusion pump
Yes No Implanted drug infusion device
Yes No Any type of prosthesis or implant
Yes No Artificial or prosthetic limb
Yes No Any metallic fragment or foreign body
Yes No Any external or internal metallic object (e.g. dentures, IUD, metal sutures)
Yes No Hearing Aid (Remove before entering the magnet room)
Yes No Tattoo
Yes No Body piercing
Yes No Other implant _____

IMPORTANT INSTRUCTIONS: Remove all metallic objects before entering the MR environment or magnet room including hearing aids, beeper, cell phone, keys, hairpins, barrettes, jewelry, watch, safety pins, paperclips, money clips, credit cards, bank cards, magnetic strip cards, coins, pens, pocket knife, nail clipper, steel-toed boots/shoes, and tools. Loose metallic objects are especially prohibited in the magnet room and MR environment.

I attest that the above information is correct to the best of my knowledge. I have read and understand the entire contents of this form and have had the opportunity to ask questions regarding the information on this form.

Person Completing Form:

Print Name Signature Date

Form Reviewed By:

Print Name Signature Date Position

WARNING: Certain implants, devices or objects may be hazardous to you in the MR environment or the magnet room. DO NOT ENTER the MR environment or the magnet room if you have any questions or concern regarding an implant, device object.

IMPORTANT INSTRUCTIONS: Remove all metallic objects before entering the MR environment or magnet room including hearing aids, beeper, cell phone, keys, hairpins, barrettes, jewelry, watch, safety pins, paperclips, money clips, credit cards, bank cards, magnetic strip cards, coins, pens, pocket knife, nail clipper, steel-toed boots/shoes, and tools. Loose metallic objects are especially prohibited in the magnet room and MR environment.

Print Name Signature Date

Form Reviewed By:

Appendix C

Pre and Post Scanning Questionnaires

Date: _____ Code:_____

Pre-Scanning Questionnaire

What time did you eat breakfast this morning?

_____

What did you eat for breakfast?

_____

Did you consume any alcohol within the last 24 hours?

_____

Did you exercise within the last 24 hours?

_____

Have you taken any over the counter medications within the past 24 hours?

_____

How well do you feel right now?

Not at all Extremely

1 2 3 4 5 6 7 8 9 10

How hungry do you feel right now?

Not at all Extremely

1 2 3 4 5 6 7 8 9 10

How sleepy do you feel right now?

Not at all Extremely

1 2 3 4 5 6 7 8 9 10

How pleasant would it be to eat right now?

Not at all Extremely

1 2 3 4 5 6 7 8 9 10

How warm do you feel right now?

Not at all Extremely

1 2 3 4 5 6 7 8 9 10

How anxious do you feel right now?

Not at all Extremely

1 2 3 4 5 6 7 8 9 10

How dizzy do you feel right now?

Not at all Extremely

1 2 3 4 5 6 7 8 9 10

How thirsty are you right now?

Not at all Extremely

1 2 3 4 5 6 7 8 9 10

How content do you feel right now?

Not at all Extremely

1 2 3 4 5 6 7 8 9 10

Appendix D

Positive and Negative Affect Schedule (PANAS)

This scale consists of a number of words that describe different feelings and emotions. Read each item and then circle the appropriate answer next to that word. Indicate to what extent you have felt this way during the past 24 hours. Use the following scale to record your answers.

(1) = Very slightly or not at all (2) = A little (3) = Moderately (4) = Quite a bit (5) = Extremely

	Very slightly or not at all	A little	Moderately	Quite a bit	Extremely
1. Interested	1	2	3	4	5
2. Distressed	1	2	3	4	5
3. Excited	1	2	3	4	5
4. Upset	1	2	3	4	5
5. Strong	1	2	3	4	5
6. Guilty	1	2	3	4	5
7. Scared	1	2	3	4	5
8. Hostile	1	2	3	4	5
9. Enthusiastic	1	2	3	4	5
10. Proud	1	2	3	4	5
11. Irritable	1	2	3	4	5
12. Alert	1	2	3	4	5
13. Ashamed	1	2	3	4	5
14. Inspired	1	2	3	4	5
15. Nervous	1	2	3	4	5
16. Determined	1	2	3	4	5
17. Attentive	1	2	3	4	5
18. Jittery	1	2	3	4	5
19. Active	1	2	3	4	5